

Safety-Critical Modular Deep Reinforcement Learning with Temporal Logic through Gaussian Processes and Control Barrier Functions

Mingyu Cai¹, Cristian-Ioan Vasile¹

Abstract—Reinforcement learning (RL) is a promising approach and has limited success towards real-world applications, because ensuring safe exploration or facilitating adequate exploitation is a challenge for controlling robotic systems with unknown models and measurement uncertainties. Such a learning problem becomes even more intractable for complex tasks over continuous state-space and action-space. In this paper, we propose a learning-based control framework consisting of several aspects: (1) linear temporal logic (LTL) is leveraged to express complex tasks over an infinite horizons which can be translated to a novel automaton structure; (2) we propose an innovative reward scheme for RL-agent with the formal guarantee such that global optimal policies maximize the probability of satisfying the LTL specifications; (3) based on a reward shaping technique, we develop a modular policy-gradient architecture utilizing the benefits of automaton structures to decompose overall tasks and enhance the performance of learned controllers; (4) by incorporating Gaussian Processes (GPs) to estimate the uncertain dynamic systems, we synthesize a model-based safeguard using Exponential Control Barrier Functions (ECBFs) to address problems with high-order relative degrees. In addition, we utilize the properties of LTL automata and ECBFs to construct a guiding process to further improve the efficiency of exploration. Finally, we demonstrate the effectiveness of the framework via several robotic environments. And we show such an ECBF-based modular deep RL algorithm achieves near-perfect success rates and guard safety with a high probability confidence during training.

Keywords—Reinforcement Learning, Deep Neural Networks, Formal Methods, Control Barrier Function, Gaussian Processes

I. INTRODUCTION

Reinforcement learning (RL) is a sequential decision-making process and focuses on learning the optimal policies that maximize the long-term reward via sampling from unknown environments [1]. Markov decision processes (MDP) are often employed to model dynamics of the interaction. Growing research has been devoted to studying RL-based motion planning over an MDP without any prior knowledge on complex robot dynamics and uncertainty models. This approach has been successfully employed in robotics where it was extended to continuous state-action spaces via actor-critic methods. [2]–[4]. However, the key feature of RL is its sole dependence on exploration of the environment. The challenge of interpreting the inner workings of many RL algorithms makes it intractable to encode the behaviors of the systems during training, especially while the learning parameters have

not yet converged to a stable control policy. The safety-critical notation refers the systems in which certain failure conditions are not tolerable and may be harmful for physical systems. Due to safety-critical requirements of real-world applications during training, any modern RL algorithm has limited success of physical systems beyond simulated applications. In this work, we propose a safety-critical control framework to address the issue of the uncertain model over continuous space integrating with the data-driven machine learning.

Safe RL is an emerging research field focusing on finding the optimal policy that maximizes the expected return while ensuring safety-critical constraints during learning process [5]. As for unknown models with noisy measurements, Gaussian processes (GPs) [6] have shown to an efficient data-driven method online validating non-parametric model with a probabilistic confidence. Recent learning-based results [7]–[9] utilizes GPs for reachability analysis and iterative predictions. Furthermore, the works [10] and [11] study Lyapunov verification for safety in terms of stability guarantees and model predictive control for safe exploration, respectively. In the field of nonlinear controls, Control Barrier Function (CBF) was introduced as a effective tool for safety-critical constraints [12]. The approach has been successfully integrated with GPs to certify learning-based control schemes while ensuring safe exploration [13], [14]. Both of them propose a GP-based safe online RL via CBF. Richard et al. [14] developed a guiding process and guaranteed the performance when applying trust region policy optimization (TRPO). However, all these works mainly focus on conventional control objectives, and not complex logic specifications. In this framework, we study the problems of safe RL from the perspective of formal methods defining high-level tasks. In addition, it is challenging to design a suitable and dense reward, especially for complex tasks [1]. Reward sparseness negatively impacts the optimal convergence of the overall learning process. Reward shaping is a common strategy to accelerate policy learning and relevant techniques are well studied in literature [15]–[17]. Recent work in [18] proposes the use of self-supervised online reward shaping to speed up learning without altering the optimal policy. To facilitate learning of complex high-level tasks, this work also designs an automatic reward shaping process to guide the agent toward the satisfaction.

A. Related Works

Formal logics embrace rich expressivity to describe robotic objectives [19]. Considering automaton-free strategies, [20],

¹Department of Mechanical Engineering, Lehigh University, Bethlehem, PA, USA. Email: <mingyu-cai, crv519>@lehigh.edu

[21] take robustness of signal temporal logic (STL) as rewards to guide RL-agents. Linear temporal logic (LTL) is leveraged as a mature tool to express complex tasks, and model checking of the MDP models commonly involves converting LTL formulas into different automaton structures e.g., deterministic finite automaton (DFA), deterministic Rabin automaton (DRA) [22], limit deterministic (generalized) Büchi automaton (LDBA or LDGBA) [23]. By taking DFA as reward machines to guide the LTL satisfaction, works [24]–[27] applied deep reinforcement learning to address high-dimensional state space. However, DFA can only define LTL tasks over finite horizons. As for infinite horizons, DRA was adopted to guide LTL satisfaction in [28]–[30], but [31] analyzes that DRA may fail to lead the RL-agent completing the missions. Instead, results [31], [32] applying LDBA as instructions of RL-agents, which only has one accepting set resulting sparser reward. Among the automatic architectures, employing LDGBA with several accepting sets for RL becomes a better choice and existing works [31], [33] leveraged it over discrete spaces. When considering continuous space, [34]–[36] incorporate deep deterministic policy gradient (DDPG) [2]. However, utilizing the standard DDPG algorithm in [34] cannot handle complex infinite-horizons tasks resulting in an unsatisfactory success rate, and [37] shows that directly applying LDGBA with deterministic policies to create product MDPs in works [35], [36] probably failing to satisfy the LTL specifications. The application of deterministic policies is crucial for high dimensional analysis especially for the continuous space, since many widely-applied deep RL methods adopt the actor-critic architecture relying on deterministic policies e.g., deep deterministic policy gradients (DDPG). Our recent letter [37] bridges the gap by designing a novel embedded automaton structure, and proposes a provably-correct modular architecture that jointly optimizes LTL sub-policies and achieves the satisfaction with high success rates. Most importantly, none of them above considers the safety-critical aspects during training.

Considering control synthesis of safe RL subject to LTL, recent works [38]–[40] either required strong assumptions about the dynamics of RL-agent (known model), or can only handle low-dimensional state or action space. As for continuous space, Li et al. [39] first combined the CBF and safe RL guided by robustness of Truncated LTL (TLTL) for satisfaction in dynamic environment, which can be also extended to integrating with GPs that relaxes the assumption of known dynamic systems. However, TLTL can only express the formulas over finite horizons. In contrast, this work mainly considers the LTL formulas over infinite horizons, where finite horizons can be regarded as a special case.

B. Contributions

In this paper, we introduce a general learning-based control architecture for satisfying high-level complex tasks captured by LTL, while safety-critical requirement is achieved during training. Our approach is realized in a policy gradient RL setting. The LTL formulas are converted to Embedded LDGBAs (E-LDGBA) to synchronously record unvisited accepting sets. A novel reward scheme is developed to guide the RL-agent

search towards the desired behaviors, based on which we create a modular DDPG to achieve goals with ideal performance. Then a safe module is presented and associated with the learning process, which can be regarded as a model-based "shield" through GPs and ECBF that can handle higher relative degrees. In particular, the ECBF compensators are synthesized online by quadratic programming based on the learned nominal model of GPs. Notably, the designed modular DDPG composed from automaton components is a distributed architecture of neural networks that can be trained synchronously during each episode. This work extends [37] in two main directions. Firstly, we consider online safety-critical control during learning process. Secondly, a RL guiding module is proposed to generate efficient explorations. To best of our knowledge, this is the first work that fully integrates automaton structures and the property of ECBF to improve exploration and enhance the optimal satisfaction. Compared with existing literature, detailed contributions are:

- From the task-perspective, this work generalizes the deep RL-based approach for LTL specification over both infinite horizons and finite horizons.
- As for the automaton-based learning, we develop an innovative automaton (E-LDGBA) structure to enable the deterministic policy for acceptance satisfaction, which allows adopting DDPG and more advanced algorithms for control over continuous space.
- On the aspect of reward scheme, we propose an automatic reward function. To improve the density of rewards, we design a reward shaping procedure without adding extra hyper-parameters, while still keeping the original optimality. The overall RL reward scheme also provides formal guarantees for maximum probability of satisfaction.
- In order to improve the success rate of learned policies, we propose a modular DDPG by utilizing the automaton states to decompose the complex task into several sub-tasks. This innovative architecture is shown to outperform the method of directly applying the standard DDPG algorithms. It's worth to point out the modular neural network structure using automaton can be easily adopted with any other advanced deep RL algorithms e.g. Soft Actor-Critic (SAC).
- To ensure safety, we incorporate GPs and ECBFs in the form of higher relative degrees, which can be efficiently solved using the quadratic programming online and provides a bounded confidence evaluation. We design a guiding procedure by integrating the violation of automaton structure and the perturbations of ECBF to facilitate the efficiency of exploration and promote the outputs of the deep RL deriving from the set of safe policies.

C. Organization

The remainder of the paper is organized as follow. In Section II, we introduce the modeling framework and formally define the problem. Section III presents a novel design of automaton structure with its benefits to reformulate the problem. In Section IV, the automatic dense reward scheme is proposed and verified to guide the RL-agent for satisfaction with maximum probability. Then a modular deep RL architecture is developed

to effectively find the approximated optimal policy over continuous space. Based on Section IV, Section V synthesizes a safety-critical methodology for the learning process with efficient guiding and safe feasibility enabled. In Section VI, the experimental results are presented. Last, Section VII concludes the paper.

II. PRELIMINARIES AND PROBLEM FORMULATION

A. Markov Decision Processes and Reinforcement Learning

The evolution of a dynamic system \mathcal{S} starting from any initial state $s_0 \in S_0$ is given by

$$\dot{s} = f(s) + g(s)a + d(s), \quad (1)$$

where $s \in S \subseteq \mathbb{R}^n$ is the state vector in the compact set S and $a \in A \subseteq \mathbb{R}^m$ is the control input. The functions $f: \mathbb{R}^n \rightarrow \mathbb{R}^n$, $g: \mathbb{R}^n \rightarrow \mathbb{R}^{n \times m}$ and $d = d' + \omega$ is a disturbance function such that $d': \mathbb{R}^n \rightarrow \mathbb{R}^n$ is locally Lipschitz continuous and ω is additive Gaussian noise. In (1), the functions f and g are known, while d is unknown.

Assumption 1. *The unknown function d has low complexity, as measured under the reproducing kernel Hilbert space (RKHS) norm [41]. d has a bounded RKHS norm with respect to known kernel k , that is $\|d_j\|_k \leq \infty$ for all $j \in \{1, \dots, n\}$, where d_j represents the j -th component of the vector function d , and $j \in \{1, \dots, n\}$.*

For most kernels used in practice, the RKHS is dense in the space of continuous functions restricted to a compact domain S . Thus, assumption 1 indicates we can uniformly approximate the continuous function d on a compact set S [6].

We abstract a robot's motion governed by the dynamical system \mathcal{S} and interaction with the environment as a continuous labeled Markov decision processes (cl-MDP) [42].

Definition 1. A cl-MDP is a tuple $\mathcal{M} = (S, S_0, A, p_S, AP, L, \cdot)$, where $S \subseteq \mathbb{R}^n$ is a continuous state space, S_0 is a set of initial states, $A \subseteq \mathbb{R}^m$ is a continuous action space, AP is a set of atomic propositions, $L: S \rightarrow 2^{AP}$ is a labeling function, and p_S represents the system dynamics. The distribution $p_S: \mathfrak{B}(\mathbb{R}^n) \times A \times S \rightarrow [0, 1]$ is a Borel-measurable conditional transition kernel such that $p_S(\cdot | s, a)$ is a probability measure of the next state given current $s \in S$ and $a \in A$ over the Borel space $(\mathbb{R}^n, \mathfrak{B}(\mathbb{R}^n))$, where $\mathfrak{B}(\mathbb{R}^n)$ is the set of all Borel sets on \mathbb{R}^n . The transition probability p_S captures the motion uncertainties of the agent.

The cl-MDP \mathcal{M} evolves by taking an action a_i at each stage i . A control policy is a sequence of decision rules $\xi = \xi_0 \xi_1 \dots$ at each time step, which yields a path $s = s_0 a_0 s_1 a_1 s_2 a_2 \dots$ over \mathcal{M} such that for each transition $s_i \xrightarrow{a_i} s_{i+1}$, a_i is generated based on ξ_i , where $s_i \xrightarrow{a_i} s_{i+1}$ denoted $p_S(s_{i+1} | s_i, a_i) > 0$.

Definition 2. A control policy $\xi = \xi_0 \xi_1 \dots$ is stationary, memoryless and deterministic if $\xi_t = \xi, \forall t \geq 0$ and $\xi: S \rightarrow A$. A policy is finite-memory if ξ is a finite state Markov chain.

A key aspect of cl-MDPs is that optimal policies may be finite-memory which leads to intractability [43]. Similarly, stochastic policies are not ideal when considering continuous

action-space. In this work, we use stationary, memoryless and deterministic policies to efficiently address synthesis problems.

In the following, we identify the dynamical system in (1) with a cl-MDP, where the state and action spaces are the same. A policy of the cl-MDP is mapped to a control input for (1) as piecewise-constant functions. Since d is an unknown function, p_S of \mathcal{M} is unknown a priori. Thus, we must learn desired policies through data.

Assumption 2. *We have access to observations of $s(t)$ and $L(s_t)$ at every time step $t \in \mathbb{Z}_{\geq 0}$.*

Given a cl-MDP \mathcal{M} , let $\Lambda: S \times A \times S \rightarrow \mathbb{R}$ denote a reward function. Given a discounting function $\gamma: S \times A \times S \rightarrow \mathbb{R}$, the expected discounted return under policy ξ starting from $s \in S$ is defined as

$$U^\xi(s) = \mathbb{E}^\xi \left[\sum_{i=0}^{\infty} \gamma^i(s_i, a_i, s_{i+1}) \cdot \Lambda(s_i, a_i, s_{i+1}) | s_0 = s \right].$$

An optimal policy ξ^* maximizes the expected return i.e.,

$$\xi^* = \arg \max_{\xi} U^\xi(s).$$

The function $U^\xi(s)$ is often referred to as the value function under policy ξ . Without information on p_S , reinforcement learning (RL) [44] can be employed as a powerful strategy to find the optimal policy. In this work, we focus on policy gradient methods employing deep neural networks to parameterize the policy model, due to their excellent performance on control problems over continuous state-space and action-space. The details are in Section IV.

B. Barrier Functions

Definition 3. An arbitrary safe set \mathcal{C} is defined by the super-level set of a continuous differential function (barrier function) $h: \mathbb{R}^n \rightarrow \mathbb{R}$,

$$\begin{aligned} \mathcal{C} &= \{s \in \mathbb{R}^n : h(s) \geq 0\}, \\ \partial\mathcal{C} &= \{s \in \mathbb{R}^n : h(s) = 0\}, \\ \text{Int}(\mathcal{C}) &= \{s \in \mathbb{R}^n : h(s) > 0\} \end{aligned} \quad (2)$$

where $\partial\mathcal{C}$ is the boundary and $\text{Int}(\mathcal{C})$ is the interior of the \mathcal{C} . The set \mathcal{C} is forward invariant for system (1) if $\forall s_0 \in \mathcal{C} \cap S_0$, the condition $s_t \in \mathcal{C}, \forall t \geq 0$, holds. System (1) is safe with respect to the set \mathcal{C} if it is forward invariant.

This framework applies barrier functions in the form $h \geq 0$ to define safe properties of a given cl-MDP. Consequently, it is assumed that any safety-critical constraint can be represented as (2). We also assume RL-agents start from initial state $s_0 \in \mathcal{C}$ such that $h \geq 0$, which indicates safety-critical constraints are not be violated at beginning.

C. Linear Temporal Logic

Linear temporal logic (LTL) is a formal language to describe high-level specifications of a system. The ingredients of an LTL formula are a set of atomic propositions, and combinations of Boolean and temporal operators. The syntax of an LTL formula is defined inductively as [19]

$$\phi := \text{true} \mid a \mid \phi_1 \wedge \phi_2 \mid \neg\phi_1 \mid \bigcirc\phi \mid \phi_1 \mathcal{U} \phi_2,$$

where $a \in AP$ is an atomic proposition, true, negation \neg , conjunction \wedge are propositional logic operators, and next, until \mathcal{U} are temporal operators. The semantics of an LTL formula are interpreted over a word, which is an infinite sequence $o = o_0 o_1 \dots$ where $o_i \in 2^{AP}$ for all $i \geq 0$, and 2^{AP} represents the power set of AP . Denote by $o \models \phi$ if the word o satisfies the LTL formula ϕ . For a infinite word o starting from state indexed 0, let $o(t), t \in \mathbb{N}$ denotes the value at step t , and $o[t:]$ denotes the word starting from step t . The semantics of LTL satisfaction are defined as [19]:

$$\begin{aligned} o &\models \text{true} \\ o &\models \pi &\Leftrightarrow \pi \in o(0) \\ o &\models \phi_1 \wedge \phi_2 &\Leftrightarrow o \models \phi_1 \text{ and } o \models \phi_2 \\ o &\models \neg \phi &\Leftrightarrow o \not\models \phi \\ o &\models \bigcirc \phi &\Leftrightarrow o[1:] \models \phi \\ o &\models \phi_1 \mathcal{U} \phi_2 &\Leftrightarrow \exists t \text{ s.t. } o[t:] \models \phi_2, \forall t' \in [0, t), o[t':] \models \phi_1 \end{aligned}$$

Alongside the standard operators introduced above, other propositional logic operators such as false, disjunction \vee , implication \rightarrow , and temporal operators always \square , eventually \diamond can be derived in LTL.

D. Problem Formulation

Given a barrier function h (or mutiple ones), the safe set is defined as $\mathcal{C} = \{s \in \mathbb{R}^n : h(s) \geq 0\}$. We can builds a connection between safe sets and LTL formulas as

Definition 4. Given a cl-MDP and a safe set \mathcal{C} , we denote by ϕ_{safe} the safety proposition for the state s of system (1). Formally, $s \models \phi_{safe}$ if and only if $s(0) \in \mathcal{C}$. The safety-critical task is defined as $\square \phi_{safe}$ such that $s(t) \in \mathcal{C}, \forall t \in \mathbb{Z}_{\geq 0}$, where $s(t)$ is the state at t .

Consider an RL-agent with dynamics \mathcal{S} and the corresponding safe set \mathcal{C} that performs a mission described by the LTL formula $\phi = \square \phi_{safe} \wedge \phi_g$. The interaction of the RL-agent with the environment is modeled by a cl-MDP $\mathcal{M} = (S, S_0, A, p_S, AP, L)$. The induced path under a policy $\xi = \xi_0 \xi_1 \dots$ over \mathcal{M} is $s_\infty^\xi = s_0 \dots s_i s_{i+1} \dots$. Let $L(s_\infty^\xi) = l_0 l_1 \dots$ be the sequence of labels associated with s_∞^ξ such that $l_i = L(s_i), \forall i \in \{1, 2, \dots\}$. Denote the satisfaction relation of the induced trace for ϕ by $L(s_\infty^\xi) \models \phi$. The probabilistic satisfaction under the policy ξ from an initial state $s_0 \in S_0$ is denoted by

$$\Pr_M^\xi(\phi) = \Pr_M^\xi(L(s_\infty^\xi) \models \phi | s_\infty^\xi \in \mathcal{S}_\infty^\xi), \quad (3)$$

where \mathcal{S}_∞^ξ is a set of admissible paths from the initial state s_0 under the policy ξ , and $\Pr_M^\xi(\phi)$ can be computed from [19].

Assumption 3. It is assumed that there exists at least one policy whose induced traces satisfy the task ϕ with non-zero probability. And there are no conflicts between ϕ_g and $\square \phi_{safe}$.

Assumption 3 indicates the existence of policies satisfying ϕ . We formulate the control learning problem as follows.

Problem 1. Given a cl-MDP $\mathcal{M} = (S, S_0, A, p_S, AP, L)$ with unknown transition probabilities p_S , and an LTL task $\phi = \square \phi_{safe} \wedge \phi_g$ with corresponding safe set \mathcal{C} ,

- (i) learn an optimal policy ξ^* that maximizes the satisfaction probability i.e., $\xi^* = \arg \max_{\xi} \Pr_M^\xi(\phi)$, in the limit,
- (ii) and maintain the satisfaction of safety-critical task $\square \phi_{safe}$ during the learning process and policy execution.

III. AUTOMATON SYNTHESIS

A. E-LDGBA

The satisfaction of the LTL formulae can be captures by limit deterministic generalized Büchi automata (LDGBA) [23]. Before defining LDGBA, we first introduce generalized Büchi automata (GBA).

Definition 5. A GBA is a tuple $\mathcal{A} = (Q, \Sigma, \delta, q_0, F)$, where Q is a finite set of states; $\Sigma = 2^{AP}$ is a finite alphabet, $\delta: Q \times \Sigma \rightarrow 2^Q$ is the transition function, $q_0 \in Q$ is an initial state, and $F = \{F_1, F_2, \dots, F_f\}$ is a set of accepting sets with $F_i \subseteq Q, \forall i \in \{1, \dots, f\}$.

Denote by $q = q_0 q_1 \dots$ a run of a GBA, where $q_i \in Q, i = 0, 1, \dots$. The run q is accepted by the GBA, if it satisfies the generalized Büchi acceptance condition, i.e., $\inf(q) \cap F_i \neq \emptyset, \forall i \in \{1, \dots, f\}$, where $\inf(q)$ denotes the set of states that repeat infinitely often in q .

Definition 6. A GBA is an LDGBA if the transition function δ is extended to $Q \times (\Sigma \cup \{\epsilon\}) \rightarrow 2^Q$, and the state set Q is partitioned into a deterministic set Q_D and a non-deterministic set Q_N , i.e., $Q_D \cup Q_N = Q$ and $Q_D \cap Q_N = \emptyset$, where

- the state transitions in Q_D are total and restricted within it, i.e., $|\delta(q, \alpha)| = 1$ and $\delta(q, \alpha) \subseteq Q_D$ for every state $q \in Q_D$ and $\alpha \in \Sigma$,
- the ϵ -transition is not allowed in the deterministic set, i.e., for any $q \in Q_D, \delta(q, \epsilon) = \emptyset$, and
- the accepting sets are only in the deterministic set, i.e., $F_i \subseteq Q_D$ for every $F_i \in F$.

To convert an LTL formula to an LDGBA, readers are referred to Owl [45]. However, previous works [37] have shown that directly using an LDGBA and deterministic policies may fail to satisfying LTL specifications due to its multiple accepting sets. Many advanced deep RL algorithms are based on the assumption that there exists at least one deterministic policy to achieve the desired objective. As a result, LDGBA can not be adopted with the DDPG algorithm. To overcome the drawback, we propose E-LDGBA and verify its expressivity as follows.

For an LDGBA \mathcal{A} , a tracking-frontier set $T \subseteq F$ is designed to keep track of unvisited accepting sets. We initialize T as to include all accepting sets, i.e. $T = F$. We abuse notation, and denote by $F(q) = \{F_j \mid q \in F_j \wedge F_j \in F\}$ the sets of accepting states that contain state q . The Boolean variable \mathcal{B} indicates the satisfaction of the accepting condition for each round. The tracking frontier $(T', \mathcal{B}) = f_V(q, T)$ is updated as

$$f_V(q, T) = \begin{cases} (T \setminus F(q), \text{false}) & \text{if } F(q) \neq \emptyset \text{ and } F_j \in T \\ (F \setminus F(q), \text{true}) & \text{if } F(q) \neq \emptyset \text{ and } T = \emptyset \\ (T, \text{false}) & \text{otherwise} \end{cases} \quad (4)$$

Definition 7 (Embedded LDGBA). Given an LDGBA $\mathcal{A} = (Q, \Sigma, \delta, q_0, F)$, its corresponding E-LDGBA is denoted by $\bar{\mathcal{A}} = (\bar{Q}, \Sigma, \bar{\delta}, \bar{q}_0, \bar{F}, f_V)$, where the tracking frontier is initially set as $T_0 = F$ s.t. $\bar{q}_0 = (q_0, T_0)$; $\bar{Q} = Q \times 2^F$ is the set of augmented states and 2^F denotes all subsets of F i.e., $\bar{q} = (q, T)$; the finite alphabet Σ is the same as the LDGBA; the transition function $\bar{\delta}: \bar{Q} \times (\Sigma \cup \{\epsilon\}) \rightarrow 2^{\bar{Q}}$ is defined such that $\bar{q}' = \bar{\delta}(\bar{q}, \bar{\sigma})$ with $\bar{\sigma} \in (\Sigma \cup \{\epsilon\})$, $\bar{q} = (q, T)$ and $\bar{q}' = (q', T')$, if it satisfies (1) $q' = \delta(q, \bar{\sigma})$, and (2) T is synchronously updated as $T' = f_V(q', T)$ after transition $\bar{q}' = \bar{\delta}(\bar{q}, \bar{\sigma})$; $\bar{F} = \{\bar{F}_1, \bar{F}_2 \dots \bar{F}_f\}$ with $\bar{F}_j = \{(q, T) \in \bar{Q} | q \in F_j \wedge F_j \subseteq T\}$ for all $j = 1, \dots, f$, is the sets of accepting states.

In Def. 7, the state-space is extended with the tracking-frontier set T that can be practically represented via one-hot encoding based on the indices of accepting sets, and is synchronously updated after each transition. Once an accepting set F_j is visited, it is removed from T , and if T is empty, it resets to $F \setminus F_j$. The accepting states of E-LDGBA ensure that progress is made towards each accepting set of the LDGBA before considering the next ones. The novel design ensures all accepting sets of original LDGBA are visited in each round under deterministic policies.

For an LTL formula ϕ , let $\bar{\mathcal{A}}_\phi$ and \mathcal{A}_ϕ be the corresponding E-LDGBA and LDGBA, respectively. Let $\mathcal{L}(\mathcal{A}_\phi) \subseteq \Sigma^\omega$ and $\mathcal{L}(\bar{\mathcal{A}}_\phi) \subseteq \Sigma^\omega$ be the accepted languages of \mathcal{A}_ϕ and $\bar{\mathcal{A}}_\phi$, respectively, over the same alphabet Σ . Based on [19], $\mathcal{L}(\mathcal{A}_\phi)$ is the set of all infinite words that satisfy LTL formula ϕ .

Lemma 1. *For any LTL formula ϕ , we can construct LDGBA $\mathcal{A}_\phi = (Q, \Sigma, \delta, q_0, F)$ and E-LDGBA $\bar{\mathcal{A}}_\phi = (\bar{Q}, \Sigma, \bar{\delta}, \bar{q}_0, \bar{F}, f_V)$. It holds that*

$$\mathcal{L}(\bar{\mathcal{A}}_\phi) = \mathcal{L}(\mathcal{A}_\phi). \quad (5)$$

Proof. See Appendix A-A. \square

Lemma 1 illustrates that both E-LDGBA and LDGBA accept the same language. Consequently, E-LDGBA can be used to ensure the satisfaction of LTL specifications.

Definition 8. A non-accepting sink component $\bar{Q}_{sink} \subseteq \bar{Q}$ of an E-LDGBA is a strongly connected directed graph with no outgoing transitions s.t. the acceptance condition can not be satisfied if starting from any state in \bar{Q}_{sink} [36]. We denote the union of all non-accepting sink components as \bar{Q}_{sinks} .

Definition 9. Given an LTL formula $\phi = \Box \phi_{safe} \wedge \phi_g$, a non-accepting unsafe component $\bar{Q}_{unsafe} \subseteq \bar{Q}_{sinks}$ of an E-LDGBA is a sink component s.t. $\bar{Q}_{unsafe} = \{(q' \in \bar{Q}) | \forall \bar{q} \in \bar{Q}, \bar{q}' = \bar{\delta}(\bar{q}, \neg \phi_{safe})\}$.

The automaton system enters into \bar{Q}_{unsafe} whenever $\Box \phi_{safe}$ is violated, which means $\phi = \Box \phi_{safe} \wedge \phi_g$ can not be satisfied anymore. The set \bar{Q}_{unsafe} can be used as an indicator of unsafety during learning process.

B. Embedded Product MDP

To satisfy a complex LTL-defined task over infinite horizons, we can define a product structure.

Definition 10. Given a cl-MDP \mathcal{M} and an E-LDGBA $\bar{\mathcal{A}}_\phi$, the EP-MDP is defined as $\mathcal{P} = \mathcal{M} \times \bar{\mathcal{A}}_\phi = (X, U^\mathcal{P}, p^\mathcal{P}, x_0, F^\mathcal{P}, \mathcal{S}, f_V)$, where $X = S \times Q \times 2^F$ is the set of product states, i.e., $x = (s, \bar{q}) = (s, q, T) \in X$; $U^\mathcal{P} = A \cup \{\epsilon\}$ is the set of actions, where the ϵ -actions are only allowed for transitions from Q_N to Q_D ; $x_0 = (s_0, \bar{q}_0)$ is the initial state; $F^\mathcal{P} = \{F_1^\mathcal{P}, F_2^\mathcal{P} \dots F_f^\mathcal{P}\}$ where $F_j^\mathcal{P} = \{(s, \bar{q}) \in X | \bar{q} \in \bar{F}_j, j \in \{1, \dots, f\}\}$; $p^\mathcal{P}$ is the transition kernel for any transition $(x, u^\mathcal{P}, x')$ with $x = (s, \bar{q})$ and $x' = (s', \bar{q}')$ such that: (1) $p^\mathcal{P}(x, u^\mathcal{P}, x') = p_S(s' | s, a)$ if $s' \sim p_S(\cdot | s, a)$, $\bar{\delta}(\bar{q}, L(s)) = \bar{q}'$ where $u^\mathcal{P} = a \in A$ (2) $p^\mathcal{P}(x, u^\mathcal{P}, x') = 1$ if $u^\mathcal{P} \in \{\epsilon\}$, $\bar{q}' \in \delta(\bar{q}, \epsilon)$ and $s' = s$; and (3) $p^\mathcal{P}(x, u^\mathcal{P}, x') = 0$ otherwise.

The EP-MDP \mathcal{P} captures the identification of admissible agent motions over \mathcal{M} that satisfy the task ϕ . Let π denote a policy over \mathcal{P} and denote by $x_\infty^\pi = x_0 \dots x_i x_{i+1} \dots$ an infinite path generated by π . Any memory-less policy π of \mathcal{P} can be projected onto \mathcal{M} to obtain a finite-memory policy ξ [19].

A path x_∞^π satisfies the acceptance condition if $\inf (x_\infty^\pi) \cap F_i^\mathcal{P} \neq \emptyset, \forall i \in \{1, \dots, f\}$, which can be denoted as $x_\infty^\pi \models \text{Acc}_p$. An accepting path satisfies the LTL task ϕ . We denote $\Pr^\pi[x_0 \models \text{Acc}_p]$ as the probability of satisfying the acceptance condition of \mathcal{P} under policy π starting from initial state x_0 , and denote $\Pr_{max}[x_0 \models \text{Acc}_p] = \max \Pr_M^\pi[x_0 \models \text{Acc}_p]$. In Problem 1, finding a policy ξ of \mathcal{M} to satisfy ϕ is equivalent to searching for a policy π of \mathcal{P} to satisfy the acceptance condition.

Remark 1. Explicitly constructing the EP-MDP is impossible over continuous space. In this work, we generate EP-MDP on-the-fly which means the approach tracks the states of an underlying structure based on Def. 10.

C. Properties of EP-MDP

A sub-MDP $\mathcal{P}_{(X', U')}$ of \mathcal{P} is a pair (X', U') where $X' \subseteq X$ and U' is a action sub-space of $U^\mathcal{P}$ such that (i) $X' \neq \emptyset$, and $U'(x) \neq \emptyset, \forall x \in X'$; (ii) $\{x' \in X' | p^\mathcal{P}(x, u, x') > 0, \forall x \in X' \text{ and } \forall u \in U'(x)\}$. The induced graph of $\mathcal{P}_{(X', U')}$ is a directed graph $\mathcal{G}_{(X', U')}$, where X' is regarded as a set of nodes, and if $p^\mathcal{P}(x, u, x') > 0$ for some $u \in U'(x)$ with $x, x' \in X'$, then there exists an edge between x and x' in $\mathcal{G}_{(X', U')}$. A sub-MDP is called a strongly connected component (SCC) if its induced graph is strongly connected, i.e., for all pairs of nodes $x, x' \in X'$, there is a path from x to x' . A bottom strongly connected component (BSCC) is an SCC from which no outside state is reachable by applying the restricted action space.

Definition 11. A Markov chain $MC_\mathcal{P}^\pi$ of the \mathcal{P} is a sub-MDP of \mathcal{P} induced by a policy π [19].

Definition 12. A sub-MDP $\mathcal{P}_{(X', U')}$ is called an end component (EC) of \mathcal{P} if its induced graph is a BSCC. An EC $\mathcal{P}_{(X', U')}$ is called a maximal end component (MEC) if there is no other EC $\mathcal{P}_{(X'', U'')}$ such that $X' \subseteq X''$ and $U'(x) \subseteq U''(x), \forall x \in X'$.

Consider a sub-MDP $\mathcal{P}_{(X', U')}$ of \mathcal{P} , where $X' \subseteq X$ and $U' \subseteq U^P$. If $\mathcal{P}_{(X', U')}$ is a maximum end component (MEC) [19] of \mathcal{P} and $X' \cap F_i^P \neq \emptyset, \forall i \in \{1, \dots, f\}$, then $\mathcal{P}_{(X', U')}$ is called an accepting maximum end component (AMEC) of \mathcal{P} . Once a path enters an AMEC, the subsequent path will stay within it by taking restricted actions from U' . Satisfying task ϕ is equivalent to reaching an AMEC [19]. Moreover, a MEC that does not intersect with any accepting sets is called a rejecting MEC (RMEC) and a MEC intersecting with only some, but not all, accepting sets is called a neutral maximum end component (NMEC).

Definition 13. [46] States of any Markov chain $MC_{\mathcal{P}}^{\pi}$ under policy π can be represented by a disjoint union of a transient class \mathcal{T}_{π} and n_R closed irreducible recurrent classes $\mathcal{R}_{\pi}^j, j \in \{1, \dots, n_R\}$, where a class is a set of states.

Under policy π , the notation \mathcal{T}_{π} represents the behaviors before entering into MECs, and \mathcal{R}_{π}^j involves the behaviors after entering into a MEC.

Lemma 2. Given an EP-MDP $\mathcal{P} = \mathcal{M} \times \mathcal{A}_{\phi}$, the recurrent class \mathcal{R}_{π}^j of $MC_{\mathcal{P}}^{\pi}, \forall j \in \{1, \dots, n_R\}$, induced by π satisfies one of the following conditions: (i) $\mathcal{R}_{\pi}^j \cap F_i^P \neq \emptyset, \forall i \in \{1, \dots, f\}$, or (ii) $\mathcal{R}_{\pi}^j \cap F_i^P = \emptyset, \forall i \in \{1, \dots, f\}$.

Proof. See Appendix A-B \square

Lemma 2 indicates that, for any policy, all accepting sets will be placed either in the transient class or in the recurrent classes. As a result, we can exclude the case of the RMEC, which simplifies the analysis of the acceptance condition.

To monitor the safety-critical requirement via automaton structure, we define the sink components of violating $\Box\phi_{unsafe}$ in an EP-MDP as:

Definition 14. Given an EP-MDP $\mathcal{P} = \mathcal{M} \times \mathcal{A}_{\phi}$, the non-accepting unsafe sink component can be defined as: $X_{unsafe} \subseteq X$ s.t. $X_{unsafe} = \{(s, \bar{q}) \in X\} \mid \bar{q} \in \bar{Q}_{unsafe}\}$.

Based on Def. 9, if the system enters X_{unsafe} , it implies the violation of the safety constraint over \mathcal{P} . Thus, Problem 1 can be reformulated as:

Problem 2. Given a user-specified LTL task $\phi = \Box\phi_{safe} \wedge \phi_g$ and a cl-MDP with unknown transition probability, the goal consists of two parts:

- (i). Find a policy π^* satisfying the acceptance condition of \mathcal{P} with maximum probability in the limit, i.e., $\Pr^{\pi^*}[\mathbf{x} \models \text{Acc}_p] = \Pr_{max}[\mathbf{x} \models \text{Acc}_p]$;
- (ii). Avoid entering X_{unsafe} during the learning process.

Section IV constructs a modular RL architecture to generate RL controllers for solving part (i) of Problem 2. Section V presents an approach to fulfill requirement (ii) of Problem 2 by proposing a GP-based ECBF compensators for the RL controllers to ensure safety during training.

IV. LEARNING-BASED CONTROL

First, Section IV-A designs a base reward scheme over the EP-MDP to guide the RL-agent to find an optimal policy satisfying the LTL task with maximum probability. In order to

improve the reward density, Section IV-B synthesizes a reward shaping process that does not change the original optimal policies. Section IV-C shows how to apply the shaped reward to construct a modular deep RL architecture to solve part (i) of Problem 2.

A. Base Reward Scheme

Let F_U^P denote the union of accepting states, i.e., $F_U^P = \{x \in X \mid x \in F_i^P, \forall i \in \{1, \dots, f\}\}$. For each transition (x, u^P, x') in the EP-MDP, the reward and discounting function only depend on current state x , i.e., $R(x, u^P, x') = R(x)$ and $\gamma(x, u^P, x') = \gamma(x)$.

Inspired by [32], we propose the reward function

$$R(x) = \begin{cases} 1 - r_F, & \text{if } x \in F_U^P, \\ 0, & \text{otherwise,} \end{cases} \quad (6)$$

and the discounting function

$$\gamma(x) = \begin{cases} r_F, & \text{if } x \in F_U^P, \\ \gamma_F, & \text{otherwise,} \end{cases} \quad (7)$$

where $r_F(\gamma_F)$ is a function of γ_F satisfying $\lim_{\gamma_F \rightarrow 1^-} r_F(\gamma_F) = 1$ and $\lim_{\gamma_F \rightarrow 1^-} \frac{1 - \gamma_F}{1 - r_F(\gamma_F)} = 0$.

Given a path $\mathbf{x}_t = x_t x_{t+1} \dots$ starting from x_t , the return is denoted by

$$\mathcal{D}(\mathbf{x}_t) := \sum_{i=0}^{\infty} R(x_{t+i}) \cdot \prod_{j=0}^{i-1} \gamma(x_{t+j}) \quad (8)$$

where $\prod_{j=0}^{-1} := 1$. Based on (8), the expected return of any state $x \in X$ under policy π can be defined as:

$$U^{\pi}(x) = \mathbb{E}^{\pi}[\mathcal{D}(\mathbf{x}_t) \mid x_t = x]. \quad (9)$$

Due to several accepting sets of the E-LDGBA, e.g., AMEC, NMEC and RMEC, if we adopt the previous reward design, the same conclusion based on (9) in [32] can not hold in our setting. Thus, we establish the following theorem which bridges the gap between probabilistic guarantees and acceptance satisfaction.

Theorem 1. Given the EP-MDP $\mathcal{P} = \mathcal{M} \times \bar{\mathcal{A}}_{\phi}$, for any state $x \in X$, the expected return under any policy π satisfies

$$\exists i \in \{1, \dots, f\}, \lim_{\gamma_F \rightarrow 1^-} U^{\pi}(x) = \Pr^{\pi}[\Diamond F_i^P], \quad (10)$$

where $\Pr^{\pi}[\Diamond F_i^P]$ is the probability that the paths starting from state x will eventually intersect a $F_i^P \in F^P$.

Proof. See Appendix A-C. \square

Next, we show how Lemma 2 and Theorem 1 can be leveraged to ensure that the RL-agent satisfies the acceptance condition of \mathcal{P} with the maximum probability.

Theorem 2. Consider an EP-MDP \mathcal{P} to an LTL formula ϕ . Based on Assumption 1, there exists a discount factor $\underline{\gamma}$, with which any optimization method for (9) with $\gamma_F > \underline{\gamma}$ and $r_F > \underline{\gamma}$ can obtain a policy $\bar{\pi}$, such that the induced run $r_{\bar{\pi}}^{\mathcal{P}}$ satisfies the accepting condition \mathcal{P} with non-zero probability.

Proof. See Appendix A-D \square

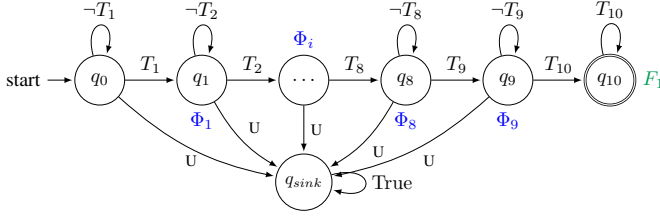


Fig. 1. LDGBA \mathcal{A}_{φ_P} has states from q_0 to q_{10} and a sink state expressing the LTL formula $\varphi_P = \Diamond(T_1 \wedge \Diamond(T_2 \wedge \Diamond \dots \wedge \Diamond T_{10})) \wedge \neg \Box U$, which requires to visit the region labeled from T_1 to T_{10} sequentially while always avoiding unsafe regions labeled as U .

Theorem 2 proves that by selecting $\gamma_F > \underline{\gamma}$ and $r_F > \underline{\gamma}$, optimizing the expected return in (9) can find a policy satisfying the given task ϕ with non-zero probability. Finally, the following conclusion of probabilistic satisfaction holds.

Theorem 3. *Given an EP-MDP \mathcal{P} , by selecting $\gamma_F \rightarrow 1^-$, the optimal policy π^* that maximizes the expected return (9) also maximizes the probability of satisfying the accepting condition, i.e., $\Pr^{\pi^*}[x_0 \models Acc_P] = \Pr_{max}[x_0 \models Acc_P]$.*

Proof. Since $\gamma_F \rightarrow 1^-$, we have $\gamma_F > \underline{\gamma}$ and $r_F > \underline{\gamma}$ from Lemma 2. There exists an induced run $r_{\mathcal{P}}^*$ satisfying the accepting condition of \mathcal{P} . According to Theorem 1, $\lim_{\gamma_F \rightarrow 1^-} U^{\pi^*}(x)$ is exactly equal to the probability of visiting the accepting sets of an AMEC. Optimizing $\lim_{\gamma_F \rightarrow 1^-} U^{\pi^*}(x)$ is equal to optimizing the probability of entering AMECs. \square

B. Dense Reward Shaping

Since the base reward function in Section IV-A is always zero for $x \notin F_U^P$, the reward signal might become sparse. To further increase the density of the reward, we propose a potential function $\Phi : X \rightarrow \mathbb{R}$, and transform the reward as:

$$R'(x, u^P, x') = R(x) + \gamma(x) \cdot \Phi(x') - \Phi(x) \quad (11)$$

Given $\mathcal{P} = \mathcal{M} \times \bar{\mathcal{A}}_\phi = (X, U^P, p^P, x_0, F^P, T, f_V, \mathcal{B})$ and the corresponding LDGBA \mathcal{A}_ϕ , let $F_U = \{q \in Q \mid q \in F_i, \forall i \in \{1, \dots, f\}\}$. For the states of \mathcal{P} whose automaton states q of $x = (s, q, T)$ belong to $Q \setminus (F_U \cup q_0 \cup Q_{sink})$ where Q_{sink} is the sink component of \mathcal{A}_ϕ , it is desirable to assign positive rewards when the agent first visits them and assign large value of reward to the accepting states to enhance the convergence of neural network. Starting from the automaton initial state, exploring any automaton state in $Q \setminus (F_U \cup q_0 \cup Q_{sink})$ can enhance the guiding of task satisfaction. To this end, an automaton tracking-frontier set T_Φ is designed to keep track of unvisited automaton components $Q \setminus (q_0 \cup Q_{sink})$, and T_Φ is initialized as $T_{\Phi 0} = Q \setminus (q_0 \cup Q_{sink})$. The set $T_{\Phi 0}$ is then updated after each transition $((s, q, T), u^P, (s', q', T))$ of \mathcal{P} as:

$$f_\Phi(q', T_\Phi) = \begin{cases} T_\Phi \setminus F(q'), & \text{if } q \in T_\Phi, \\ T_{\Phi 0} \setminus F(q') & \text{if } \mathcal{B} = \text{True}, \\ T_\Phi, & \text{otherwise.} \end{cases} \quad (12)$$

where $F(q')$ is the same as (4). The set T_Φ will only be reset when \mathcal{B} in f_V becomes True, indicating that all accepting sets in the current round have been visited. Then the potential function $\Phi(x)$ for $x = (s, q, T)$ is constructed as:

$$\Phi(x) = \begin{cases} \eta_\Phi \cdot (1 - r_F), & \text{if } q \in T_\Phi, \\ 0, & \text{otherwise} \end{cases} \quad (13)$$

where $\eta_\Phi > 0$ is the shaping parameter. Intuitively, the value of potential function for unvisited and visited states in $T_{\Phi 0}$ is equal to $\eta_\Phi \cdot (1 - r_F)$ and 0 respectively, which will enforce the efficiency of exploration.

Example 1. As a running example of the reward shaping technique. Fig. 1 shows an LDGBA of the LTL formula $\varphi_P = \Diamond(T_1 \wedge \Diamond(T_2 \wedge \Diamond \dots \wedge \Diamond T_{10})) \wedge \neg \Box U$ with only one accepting set. Let's denote any state of EP-MDP with the same automaton component and an arbitrary MDP state as $x([s], q, T)$, where the MDP component can be different. For a trajectory $x = ([s], q_0, T) u_0^P([s], q_1, T) u_1^P([s], q_2, T) u_2^P([s], q_3, T)$, the associated shaped reward for each transition is equal to $\eta_\Phi \cdot (1 - r_F)$, instead of zero.

Given a path $x_t = x_t x_{t+1} \dots$ starting from x_t associated with the corresponding action sequence $u_t^P = u_t^P u_{t+1}^P \dots$, the return can be reformulated by applying (11) as:

$$\mathcal{D}'(x_t) := \sum_{i=0}^{\infty} R(x_{t+i}, u_{t+i}^P, x_{t+i+1}) \cdot \prod_{j=0}^{i-1} \gamma(x_{t+j}) \quad (14)$$

Also, the shaped expected return of any state $x \in X$ under policy π can be

$$U'^\pi(x) = \mathbb{E}^\pi[\mathcal{D}'(x_t) \mid x_t = x]. \quad (15)$$

Proposition 1. *Given a cl-MDP \mathcal{M} and an E-LDGBA $\bar{\mathcal{A}}_\phi$, by selecting $\gamma_F \rightarrow 1^-$, the optimal policy π^* that maximizes the expected return in (15) by applying the shaped reward (11) in the corresponding EP-MDP also maximizes the probability of satisfying ϕ , i.e., $\Pr^{\pi^*}[x_0 \models Acc_P] = \Pr_{max}[x_0 \models Acc_P]$.*

Proof. The work of [15] has shown that optimizing the expected return (15) using the shaped reward (11) is equivalent to optimizing (9) with the base reward scheme, and the generated optimal policies from these two forms are the same. According to Theorem 3, one has the result. \square

Next, we take the above reward design into a deep policy gradient RL algorithm to effectively find the optimal policy over continuous space.

C. Modular Deep RL

The objective of policy-based RL attempts to find the optimal policy that maximizes the long-term expected return (15). There are several common methods: (i) policy iteration, (ii) derivative-free optimization, (iii) deep policy gradient (DPG). This work can be adopted to any of them. To address the MDPs with continuous state-action space, we implement the deep deterministic policy gradient (DDPG) algorithm [2].

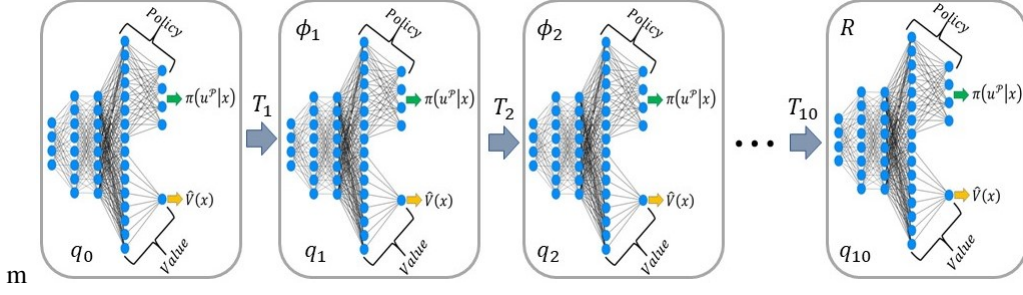


Fig. 2. Example of modular architecture based on reward shaping for the LTL formula φ_P . The distributed actor-critic neural networks are constructed based on the automata components and are learned synchronously online.

Different from directly adopting the DDPG, this framework proposes a modular architecture to improve the performance of satisfying complex tasks and reduce the global variance of the policy gradient algorithm. Its general idea is to divide the LTL task into several sub-tasks based on the automaton structure and apply several DDPG for each sub-task.

The basics of DDPG is to approximate the current deterministic policy via a parameterized function $\pi(x|\theta^u)$ called actor. The actor is a deep neural network whose set of weights are θ^u . The critic function also applies a deep neural network with parameters θ^Q to approximate action-value function $Q(x, u^P|\theta^Q)$, which is updated by minimizing the following loss function:

$$L(\theta^Q) = \mathbb{E}_{s \sim \rho^\beta} \left[(y - Q(x, \pi(x|\theta^u)|\theta^Q))^2 \right]. \quad (16)$$

The actor can be updated by applying the chain rule to the expected return with respect to actor parameters θ^u as the following policy gradient theorem:

$$\begin{aligned} \nabla_{\theta^u} U^u(x) &\approx \mathbb{E}_{s \sim \rho^\beta} [\nabla_{\theta^u} Q(x, \pi(x|\theta^u)|\theta^Q)] \\ &= \mathbb{E}_{s \sim \rho^\beta} [\nabla_{u^P} Q(x, u^P|\theta^Q) |_{u^P=\pi(x|\theta^u)} \nabla_{\theta^u} \pi(x|\theta^u)]. \end{aligned} \quad (17)$$

The complex LTL task ϕ can be divided into simple composable modules. Each state of the automaton in the LDGBA is a module and each transition between these automaton states is a "task divider". In particular, given ϕ and its LDGBA \mathcal{A}_ϕ , we propose a modular architecture of $|Q|$ DDPG respectively, i.e., $\pi_{q_i}(x|\theta^u)$ and $Q_{q_i}(x, u^P|\theta^Q)$ with $q_i \in Q$, along with their own replay buffer. Experience samples are stored in each replay modular buffer B_{q_i} in the form of $(x, u^P, R(x), \gamma(x), x')$. By dividing the LTL task into sub-stages, the set of neural nets acts in a global modular DDPG architecture, which allows the agent to jump from one module to another by switching between the set of neural nets based on transition relations of \mathcal{A}_ϕ .

Example 2. Continuing with example 1, Fig. 2 shows the modular DDPG architecture corresponding to the LTL formula φ_P based on the reward shaping scheme, where each pair of actor critic neural networks represents the standard DDPG structure along with an automaton state, and the transitions of them are consistent with the LDGBA structure.

Remark 2. In the modular architecture, instead of dividing

complex tasks by the states of E-LDGBA that has more automaton states \bar{Q} due to the embedded frontier set, we decompose the overall task based on the more compact set of states Q of LDGBA, which sparsifies the number of distributed pairs of actor-critic. Such a design reduces the complexity of memories, and achieves the same objective.

The proposed method to solve a continuous MDP with LTL specifications is summarized in Alg. 1. Line (7-11) and line (12-15) represent the learning process with and without safe leaning enabled. Details of safe learning and exploration guiding are introduced in V. Instead of constructing the EP-MDP priori, product states of EP-MDP are synchronized on-the-fly (line 9 and line 13). We assign each DDPG an individual replay buffer B_{q_i} and a random process noise N_{q_i} . The corresponding weights of modular networks, i.e., $Q_{q_i}(x, u^P|\theta^{Q_{q_i}})$ and $\pi_{q_i}(x|\theta^{u_{q_i}})$, are also updated at each iteration (line 17-20). All neural networks are trained using their own replay buffer, which is a finite-sized cache that stores transitions sampled from exploring the environment. Since the direct implementation of updating target networks can be unstable and divergent [47], the soft update (20) is employed, where target networks are slowly updated via relaxation (line 20). Note that for each iteration we first observe the output of the shaped reward function R' , then execute the update process via f_V and f_Φ (line 14-16).

Theorem 4. Given a cl-MDP \mathcal{M} and an E-LDGBA $\bar{\mathcal{A}}_\phi$, the optimal policy π^* generated from modular DDPG by applying the shaped reward (11) maximizes the probability of satisfying ϕ in the limit i.e., $\Pr^{\pi^*}[x_0 \models Acc_P] = \Pr_{max}[x_0 \models Acc_P]$.

Proof. Theorem 4 is directly derived from Proposition 1. \square

Theorem 3 and Proposition 1 assume that all state-action values can be exactly optimized, which is not in practical when considering continuous space. As for DNNs, we have to stop the training after finite number of steps in practice and the synthesised policy derived from this nonlinear regression process might be sub-optimal with respect to the true π^* as in Theorem 4. It's also worth to note that our algorithm can be easily extended with other advanced off-policy algorithms e.g. soft actor-critic (SAC) [48].

V. SAFE LEARNING AND EXPLORATION GUIDING

This Section focuses on adding the safety guard as a "shield" during learning process. First, Section V-A introduces GPs to

Algorithm 1 Safe modular DDPG

1: **procedure** INPUT: (Dynamic system \mathcal{S} , LDGBA \mathcal{A}_ϕ)
 Output: modular DDPG for optimal policy π^*
 Initialization: $|Q|$ actor $\pi_{q_i}(x|\theta^{u_{q_i}})$ and critic networks $Q_{q_i}(x, u^P|\theta^{Q_{q_i}})$ with arbitrary weights $\theta^{u_{q_i}}$ and $\theta^{Q_{q_i}}$ for all $q_i \in Q$; $|Q|$ corresponding target networks $\pi'_{q_i}(x|\theta^{u'_{q_i}})$ and $Q'_{q_i}(x, u^P|\theta^{Q'_{q_i}})$ with weights $\theta^{u'_{q_i}}$ and $\theta^{Q'_{q_i}}$ for each $q_i \in Q$, respectively; $|Q|$ replay buffers B_{q_i} ; $|Q|$ random processes noise N_{q_i}
 2: set maximum episodes E and iteration number τ
 3: **Repeat** Each Episode
 4: sample an initial state s_0 of \mathcal{M} and q_0 of \mathcal{A}_ϕ as s_t, q_t
 5: **while** $t \leq \tau$ **do**
 6: select action $u_t^P = \pi_{q_t}(x|\theta^{u_{q_t}}) + R_{q_t}$.
 7: **if** ECBF-based Safe learning enabled **then**
 8: set $a_{RL}(s_t) = u_t^P$ and obtain $a_{Safe}(s_t)$ via QP (26)
 9: execute $a_{Safe}(s_t)$ and observe
 $x_{t+1} = (s_{t+1}, q_{t+1}, T), R' \left(x_t, u_t^P, x_{t+1} \right), \gamma(x_{t+1})$
 10: execute three-step safe guiding process in Def. 17:
 $x_{t+1} = (s_{t+1}, q_{t+1}, T), R_{CBF} \left(x_t, u_t^P, x_{t+1} \right)$
 11: store the transition information in replay buffers B_{q_t} :
 $\left(x_t, a_{RL}(s_t), R_{CBF} \left(x_t, u_t^P, x_{t+1} \right), x_{t+1} \right)$
 12: **else**
 13: execute u_t^P and observe
 $x_{t+1} = (s_{t+1}, q_{t+1}, T), R' \left(x_t, u_t^P, x_{t+1} \right), \gamma(x_{t+1})$
 14: store the transition information in replay buffers B_{q_t} :
 $\left(x_t, u_t^P, R' \left(x_t, u_t^P, x_{t+1} \right), x_{t+1} \right)$
 15: **end if**
 16: execute the updates via $f_V(q_{t+1}, T)$ and $f_\Phi(q_{t+1}, T_\Phi)$
 17: calculate target values for each $i \in N$ (mini-batch sampling of B_{q_t}) as:
 $y_i = R' \left(x_i, u_i^P, x_{i+1} \right) + \gamma(x_i) \cdot Q'_{q_{i+1}} \left(x_{i+1}, u_{i+1}^P \middle| \theta^{Q'_{q_{i+1}}} \right)$
 18: update weights $\theta^{Q_{q_t}}$ of critic neural network $Q_{q_t}(x, u^P|\theta^{Q_{q_t}})$ by minimizing the loss function:

$$L = \frac{1}{N} \sum_{i=1}^N \left(y_i - Q_{q_t} \left(x_i, u_i^P \middle| \theta^{Q_{q_t}} \right) \right)^2$$

 19: update weights $\theta^{u_{q_t}}$ of actor neural network $\pi_{q_i}(x|\theta^{u_{q_t}})$ by maximizing the policy gradient:

$$\nabla_{\theta^{u_{q_t}}} U^{q_t} \approx \frac{1}{N} \sum_{i=1}^N \left(\nabla_{u^P} Q_{q_t} \left(x_i, u^P \middle| \theta^{Q_{q_t}} \right) \Big|_{u^P = \pi_{q_t}(x_i|\theta^{u_{q_t}})} \cdot \nabla_{\theta^{u_{q_t}}} \pi_{q_t}(x_i|\theta^{u_{q_t}}) \right)$$

 20: soft update of target networks:

$$\begin{aligned} \theta^{u'_{q_t}} &\leftarrow \tau \theta^{u_{q_t}} + (1 - \tau) \theta^{u'_{q_t}} \\ \theta^{Q'_{q_t}} &\leftarrow \tau \theta^{Q_{q_t}} + (1 - \tau) \theta^{Q'_{q_t}} \end{aligned}$$

 21: **end while**
 22: **Until** End of trial
 23: **end procedure**

approximate the unknown model in (1). Then Section V-B provides a continuous form of exponential control barrier functions (ECBF) for higher relative degrees, which can be incorporated with GPs to safeguard with a bounded probability. Section V-C integrates the GP-based ECBF compensators for control laws generated from the modular RL policy in Section IV-C to ensure the safety-critical requirements during learning process. To improve the efficiency of exploration and prevent the original formal optimality, Section V-D proposes an automaton-based guiding strategy that enhances RL policies being explored within the set of safe policies during training.

A. Gaussian Processes

Gaussian processes (GPs) are a non-parametric regression method to approximate the unknown system dynamics and their uncertainties from data [49]. As for the unknown disturbance function of a nonlinear map $d(s) : S \rightarrow \mathbb{R}^n$ in (1) we make use of GP regression. Informally, a GP is a distribution over functions, and each component $d_i(s)$ of n -dimensional $d(s)$ can be approximated by a GP distribution denoted as \mathcal{GP} with a mean function $u_i(s)$ and a covariance kernel function $k_i(s, s')$ as $d_i(s) \sim \mathcal{GP}(u_i(s), k_i(s, s'))$, where $k_i(s, s')$ measures similarity between any two states. The class of the prior mean function and covariance kernel function is selected to characterize the model. Then the approximation of $d(s)$ with n independent GPs is given:

$$\hat{d}(x) = \begin{cases} \hat{d}_1(s) \sim \mathcal{GP}(u_1(s), k_1(s, s')) \\ \vdots \\ \hat{d}_n(s) \sim \mathcal{GP}(u_n(s), k_n(s, s')) \end{cases}$$

Based on assumption 2, given a set of N_m input data $\{(s^{(1)}, a^{(1)}), \dots, (s^{(N_m)}, a^{(N_m)})\}$, and corresponding measurements $\{y^{(1)}, \dots, y^{(N_m)}\}$ subject to additive Gaussian noise $w \sim \mathcal{N}(\mathbf{0}_n, \sigma_{noise}^2 \mathbf{I}_n)$, where $y^{(i)} = f(s^{(i)}) + g(s^{(i)})a^{(i)} + d((s^{(i)})) + \omega^{(i)}, \forall i \in \{(1, \dots, (N_m))\}$, the mean \hat{u}_i and covariance σ_{u_i} of posterior distribution for $d_i, i \in \{(1, \dots, n)\}$ at an arbitrary query state $s_* \in S$ can be calculated as:

$$\hat{u}_i(s_*) = \hat{k}_i^T (K_i + \sigma_{noise}^2 \mathbf{I}_{N_m})^{-1} y_i$$

$$\hat{\sigma}_i^2(s_*) = k_i((s_*, (s_*) - \hat{k}_j^T (K_j + \sigma_{noise}^2 \mathbf{I}_{N_m})^{-1} \hat{k}_i$$

where $\hat{k}_i = [k_i(s^{(1)}, s_*), \dots, k_i(s^{(N_m)}, s_*)]^T$, $y_i = [(y_i^{(1)}, \dots, y_i^{(N_m)})]$ with $y_i^{(N_m)}$, and $K_i \in \mathbb{R}^{N_m \times N_m}$ is a kernel matrix s.t. $K_i^{(jl)} = k_i(s^{(j)}, s^{(l)})$ with $j, l \in \{(1, \dots, N_m)\}$.

Then we can describe the evaluation of uncertain dynamics $d(s)$ by a bounded estimation with probability $(1 - \delta)^n$ as:

$$\Pr \{u(s) - k_\delta \sigma(s) \leq d(s) \leq u(s) + k_\delta \sigma(s)\} \geq (1 - \delta)^n \quad (18)$$

where $\Pr\{\cdot\}$ represents the probability measurement, $u(s) = [\hat{u}_1(s), \dots, \hat{u}_n(s)]^T$, $\sigma(s) = [\hat{\sigma}_1(s), \dots, \hat{\sigma}_n(s)]^T$, and k_δ is a design parameter determining δ . The $d(s)$ is estimated over a multivariate GP. Note that applying GPs for large amounts of training data is intractable and problematic due to the expensive matrix computation in (18). However, this work alleviates such an issue via the episodic sampling method [14]. Any other methods for the model estimation can be also

applied into this framework. The main advantage of applying GPs compared with the feedforward neural network is the quantifiable confidence of predictions.

B. Probabilistic Exponential Control Barrier Function

For the continuous nonlinear systems, control barrier function (CBF) is an efficient tool for maintaining safety [12]. We directly apply the previous result to define the first order CBF.

Definition 15. Consider a system \mathcal{S} in (1) and assume $d(x)$ is known, and the safe set $\mathcal{C} \subseteq S$ with a continuous differentiable (barrier) function $h : S \rightarrow \mathbb{R}$ in (2). If $\frac{\partial h}{\partial s} \neq 0$ for all $s \in \partial \mathcal{C}$ and there exists an extended \mathcal{K} function α s.t.

$$L_f h(s) + L_g h(s)a + L_d h(s) \geq -\alpha(h(s)). \quad (19)$$

Then for a trajectory $s = s_0 \dots s_{N_s}$ of system (1) starting from any $s_0 \in \mathcal{C}$ under controllers satisfying (19), one gets $s_i \in \mathcal{C} \forall i \in \{0, \dots, N_s\}$. And h is a continuous CBF for (1) with respect to the safe invariant set \mathcal{C} .

For the continuous differentiable function h of the system \mathcal{S} with high relative degree $r_b \geq 1$, denote $f'(s) = f(s) + d(s)$ and one has r_b^{th} time-derivative of $h(s)$:

$$h^{(r_b)}(s) = L_f^{r_b} h(s) + L_g L_{f'}^{r_b-1} h(s)a.$$

Defining a traverse variable as

$$\begin{aligned} \xi_b &= [h(s), \dot{h}(s), \dots, h^{(r_b-1)}(s)]^T \\ &= [h(s), L_{f'} h(s), \dots, L_{f'}^{r_b-1} h(s)]^T, \end{aligned}$$

a linearized system of \mathcal{S} can be formulated:

$$\begin{aligned} \dot{\xi}_b(s) &= A_b \xi_b(s) + B_b u \\ h(s) &= C \xi_b(s) \end{aligned}$$

where

$$A_b = \begin{bmatrix} 0 & 1 & 0 & \dots & 0 \\ 0 & 0 & 1 & \dots & 0 \\ \vdots & \vdots & \vdots & \ddots & \vdots \\ 0 & 0 & 0 & \dots & 1 \\ 0 & 0 & 0 & 0 & 0 \end{bmatrix}, \quad B_b = \begin{bmatrix} 0 \\ 0 \\ \vdots \\ 0 \\ 1 \end{bmatrix},$$

and $u = L_{f'}^{r_b} h(s) + L_g L_{f'}^{r_b-1} h(s)a$ is the input-output linearized control. The lineized form allows to extend the CBFs for higher relative degrees, Exponential CBF (ECBF) [50].

Definition 16. Consider a system \mathcal{S} in (1) and assume $d(x)$ is known, and the safe set $\mathcal{C} \subseteq S$ with a continuous differentiable (barrier) function $h : S \rightarrow \mathbb{R}$ in (2) that has relative degree $r_b \geq 1$. $h(s)$ is an ECBF if there exists $K_b \in \mathbb{R}^{1 \times r_b}$ s.t.

$$L_{f'}^{r_b} h(s) + L_g L_{f'}^{r_b-1} h(s)a + K_b \xi_b \geq 0 \quad (20)$$

Then the system \mathcal{S} is forward invariant in \mathcal{C} if starting from $s_0 \in \mathcal{C}$, there exists a ECBF $h(s)$ and controllers satisfying (20) are applied.

Remark 3. The row vector K_b should be selected to render a stable close-loop matrix $A_b - B_b K_b$. Moreover, for $r_b > 1$, ECBF is a special case of general forms of Higher Order Control Barrier Function (HOCBF) [51] and the HOCBF can be easily adopted into this framework.

Now, we can relax the assumption that one has the full knowledge of the system, and extend results to the unknown system described in Section II-A by incorporating GPs. Specifically, the unknown part $d(x)$ is approximated by the learned GP model with mean $u(s)$, covariance $\sigma(s)$ and k_δ as in (18). Let's denote $\hat{f}(s)$ as estimation of the function $f'(s)$ e.g., $\hat{f}(s) = f(s) + \hat{d}(s)$, where $\hat{d}(s) \in [u(s) - k_\delta, u(s) + k_\delta]$. The GP-based traverse variable can be represented as: $\hat{\xi}_b = [h(s), L_{\hat{f}} h(s), \dots, L_{\hat{f}}^{r_b-1} h(s)]^T$. We can propose the GP-based ECBF for the nominal system.

Theorem 5. Consider a system \mathcal{S} in (1) with unknown $d(x)$ and sets $\mathcal{C} \subseteq S$ with a differentiable (barrier) function $h : S \rightarrow \mathbb{R}$ s.t. $\forall s \in \mathcal{C}, h(s) \geq 0$, if there exists a close-loop stable K_b s.t.

$$L_{\hat{f}}^{r_b} h(s) + L_g L_{\hat{f}}^{r_b-1} h(s)a + K_b \hat{\xi}_b \geq 0, \quad (21)$$

Then starting from any $s_0 \in \mathcal{C}$, controllers of the system \mathcal{S} satisfying (21), render the set \mathcal{C} forward invariant with probability at least $(1 - \delta)^n$.

Proof. Since $\hat{d}(s) \in [u(s) - k_\delta, u(s) + k_\delta]$, one has

$$\Pr \left\{ F(s, a) + \mathcal{GP}_l \leq \hat{F}(s, a) \leq F(s, a) + \mathcal{GP}_h \right\} \geq (1 - \delta)^n$$

where $F(s, a) = f(s) + g(s)a$, $\hat{F}(s, a) = F(s, a) + \hat{d}(s)$, $\mathcal{GP}_l = u(s) - k_\delta \sigma(s)$, and $\mathcal{GP}_h = u(s) + k_\delta \sigma(s)$. Then we can obtain the conclusion:

$$\Pr \left\{ L_{\hat{f}}^{r_b} h(s) + L_g L_{\hat{f}}^{r_b-1} h(s)a + K_b \hat{\xi}_b \geq 0 \right\} \geq (1 - \delta)^n. \quad \square$$

Next, we can formulate the relaxed ECBF condition of (21) into the following quadratic program (QP):

$$\begin{aligned} (a_{CBF}, \epsilon) &= \arg \min_{a, \epsilon} \left(\frac{1}{2} a^T H(s) a + K_\epsilon \epsilon \right) \\ \text{s.t. } & L_{\hat{f}}^{r_b} h(s) + L_g L_{\hat{f}}^{r_b-1} h(s)a + K_b \hat{\xi}_b + \epsilon \geq 0 \\ & a_{low}^{(i)} \leq a^{(i)} \leq a_{high}^{(i)}, i \in \{(0, \dots, n)\}, \end{aligned} \quad (22)$$

where $H(s)$ is a positive definite matrix (pointwise in s) $a_{low}^{(i)}$ and $a_{high}^{(i)}$ represent the lower bound and higher bound of each element of the control input. To ensure the existence of solutions for the QP, ϵ is a relaxation variable, and K_ϵ is a large value parameter that penalizes the safety violations. The solution of the ECBF-QP enforces the safe condition with the min-norm form (minimum control energy).

Lemma 3. For dynamic system (1) with unknown $d(s)$ and $s_0 \in \mathcal{C} = \{s \in \mathbb{R}^n : h(s) \geq 0\}$,

(i) feasible solutions of (22) for all $s \in S$ with $\epsilon = 0$ renders safe set \mathcal{C} forward invariant with probability $(1 - \delta)^n$.

(ii) feasible solutions of (22) for all $s \in S$ with $\epsilon_{high} \geq \epsilon > 0$ approximately renders safe set $\mathcal{C}_\epsilon = \left\{ s \in \mathbb{R}^n : h_\epsilon = h(s) + \frac{\epsilon_{high}}{\eta} \geq 0 \right\}$ with probability $(1 - \delta)^n$.

Proof. For part (i), since $\epsilon = 0$, the feasible solutions of (18) strictly follows the ECBF condition in theorem 5, and it provides the probabilistic bound $(1 - \delta)^n$ of the GP model (18).

For part (ii), we can utilize the discrete-time system \mathcal{S}_d as an approximately form of (1) given the sampling time Δt , and the safe set in (2) can be estimated as \mathcal{C}_d over \mathcal{S}_d . Inspired by [52], there exists a discrete-time ECBF h_d with $\eta \in (0, 1]$ that renders the set invariant as:

$$h_d(\hat{F}(s_t, a)) \geq (1 - \eta) h_d(s_t), \quad (23)$$

Then the constraint $h_d(\hat{F}(s_t, a)) \geq (1 - \eta) h_d(s_t) + \epsilon$ in (22) can be reformulated as:

$$h_d(\hat{F}(s_t, a)) + \frac{\epsilon_{high}}{\eta} \geq 0 \geq (1 - \eta) (h_d(s_t) + \frac{\epsilon_{high}}{\eta}). \quad (24)$$

This equation and theorem 5 conclude the proof. \square

Note that constructing the accurate discrete-time ECBF over \mathcal{S}_d for general safe requirements is challenging even if there exists one, and lemma 3 theoretically applies it to evaluate the performance of the relaxed ECBF-QP.

Remark 4. One can easily extend the framework for the data-driven based barrier functions [53], [54]. This work focuses on efficient safe learning for the optimal policy that satisfies high-level LTL over infinite horizons and bypass the consideration of unknown ECBFs. Also we can combine multiple ECBFs as constraints into (22) to define complex safe regions.

C. ECBF-Based Safe Learning

Before developing the safety-critical methodology, it's reasonable to show that there's no conflicts between safe exploration and optimal policies generated from Section IV.

Lemma 4. Given the LTL formula as the form of $\phi = \Box \phi_{safe} \wedge \phi_g$ defined in Section II-C, let π_{opt} denotes the optimal policy obtained from Section IV and π_{safe} denotes a set of all safe policies satisfying $\Box \phi_{safe}$. One has the property $\pi_{opt} \subseteq \pi_{safe}$.

Lemma 4 can be straightly proved according to the fact that $\Box \phi_{safe}$ is encoded into a part of LTL objective ϕ , and π_{opt} is verified to satisfy ϕ . This relationship is shown in Fig. 3.

During the learning process, let $x_t = (s_t, \bar{q}_t)$ and π_t denote product state and learning policy at time-step t respectively. And u_t^P is the action obtained based on the policy π_t e.g. $u_t^P \sim \pi_t$. According to Def. 10, one has the action of \mathcal{M} as

$$a_{RL}(s_t) = \begin{cases} u_t^P, & \text{if } u_t^P \notin \{\epsilon\}, \\ 0, & \text{otherwise,} \end{cases} \quad (25)$$

The controller for any state s during training can be generated based on (25) as $a_{RL}(s_t)$. However, such a controller may not be safe. To overcome the issue, one builds the QP according to GP-based ECBF in (22) as a safeguard module to provide the minimal perturbation $a_{pt}(s_t)$ for the original control $a_{RL}(s)$.

$$\begin{aligned} (a_{pt}, \epsilon) &= \arg \min_{a, \epsilon} \frac{1}{2} (a_{RL}(s) + a)^T H(s) (a_{RL}(s) + a) + K_\epsilon \epsilon \\ \text{s.t. } & L_f^{r_b} h(s) + L_g L_f^{r_b-1} h(s) (a_{RL}(s) + a) + K_b \hat{\xi}_b + \epsilon \geq 0 \\ & a_{low}^{(i)} \leq (a_{RL}(s) + a)^{(i)} \leq a_{high}^{(i)}, i \in \{(0, \dots, n)\}, \end{aligned} \quad (26)$$

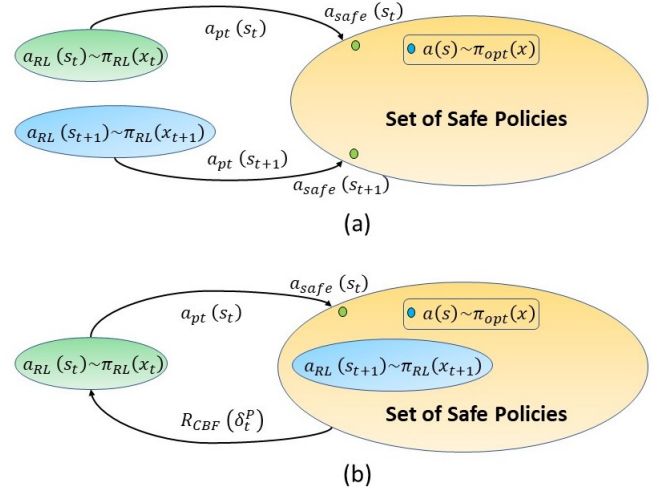


Fig. 3. Illustration of the effective improvement of exploration guiding. (a) Policy optimization without enforcing exploration that the RL policies receive no information related to the safe requirements. (b) Policy optimization with automaton-based guiding to enforce the RL policy generated within the set of safe policies.

Consequently, the actual implemented safety-critical controllers can be formulated from (26) as:

$$a_{Safe}(s) = a_{RL}(s) + a_{pt}(s) \quad (27)$$

During the evolution of the dynamic system (1), the "shield" of (26) compensates the model-free RL controller $a_{RL}(s)$ based the GP-based ECBF condition, and keeps the state safe via deploying the final safe controller $a_{Safe}(s)$.

However, purely combining GPs and ECBF during learning process may negatively influence the exploration for original optimal convergence as verified in Section IV. Since the optimal parameterized RL-policy π^* of the controller $a_{RL}(s)$ attempts to optimize the expected return and π^* is generated based on the distribution of the policy-gradient optimization in (17), the feedback reward at each time should correspond to the controller $a_{RL}(s)$. While the actual reward collection in reply buffer is associated to the controller $a_{CBF}(s)$, which is not consistent with the RL-policy π^* inducing undesired behaviors. As a result, the modular DDPG receives no informative feedback about the unsafe behaviors compensated from (26). Moreover, another crucial issue is that the functionality of $a_{Safe}(s)$ is too monotonous to guide the policy exploration and the corresponding RL policy π^* may always being around the margins of unsafe sets, as illustrate in Fig. 3 (a).

D. Exploration Guiding

In order to achieve safe and efficient guiding, the work [14] estimates the previous history of CBF perturbations to improve the efficiency of the learning process. However, such a design may negatively impact the exploration of applying DDPG for original optimal policies proposed in Section IV, and it can not provide formal guarantees on the aspect of LTL satisfaction.

To overcome the intrigued challenges, this section proposes an automaton-based guiding process combining the properties of E-LDGBA and ECBF. Given an LTL formula as the form

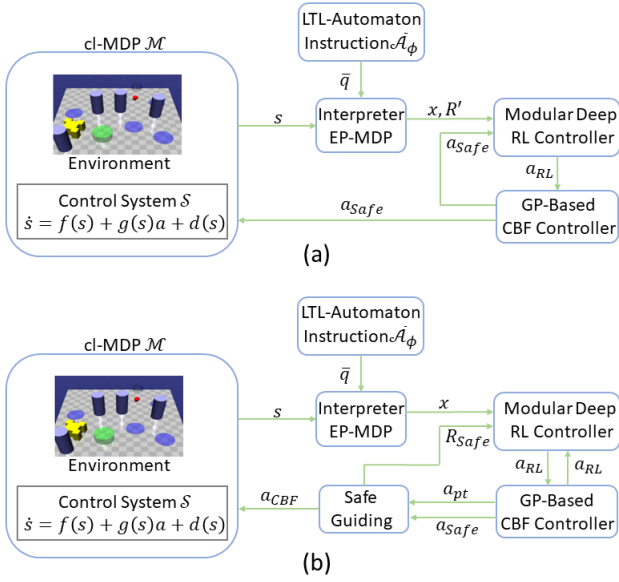


Fig. 4. Control synthesis integrates with the modular RL controllers and GP-based CBF controllers. (a) Modular RL architecture that directly uses the CBF-based safe controllers without enforcing exploration. (b) Framework enabled with techniques of safe guiding and improvement of learning efficiency.

$\phi = \square\phi_{safe} \wedge \phi_g$ where $\square\phi_{safe}$ is the specification to render the safe set \mathcal{C} forward invariant, the intuition for (27) is that $a_{pt}(s) \neq 0$ implies the unsafe RL controller $a_{RL}(s)$, which violates the $\square\phi_{safe}$ of ϕ . Consequently, the objective of efficient exploration is to encourage the RL-agent operating in the safe region \mathcal{C} , and to enforce $a_{pt}(s)$ decaying to zero.

Recall during the learning process, one has $x_t = (s_t, \bar{q}_t)$, π_t at time-step t , and obtains $a_{RL}(s_t)$ as (25) from corresponding $u_t^P \sim \pi_t$. Then applying GP-based QP (26) generates $a_{pt}(s_t)$ and $a_{Safe}(s_t)$. The next state $x_{t+1} = (s_{t+1}, \bar{q}_{t+1})$ can be generated by taking the safe action $a_{Safe}(s_t)$ s.t. $p_S(s_{t+1}|s_t, a_{Safe}(s_t)) \neq 0$ and $\bar{q}_{t+1} = \bar{\delta}(\bar{q}_t, L(s_t))$. The automaton-based safe guiding consists of three steps: ECBF-based reward shaping, violation-based automaton updating, and relay buffer switching. The procedure of safe guiding is shown in Fig. 4 (b), compared with the method of directly integrating the safe execution in Fig. 4 (a).

Definition 17. Given the transition $\delta_t^P = (x_t, a_{Safe}(s_t), x_{t+1})$, where $x_t = (s_t, \bar{q}_t)$, $a_{RL}(s_t)$ is obtained from $u_t^P \sim \pi_t$ as (25), $a_{Safe}(s_t) = a_{RL}(s_t) + a_{pt}(s_t)$, and $x_{t+1} = (s_{t+1}, \bar{q}_{t+1})$ generated based on Def. 10 during learning process, the three-step exploration guiding can be defined as:

- (1) The reward is shaped based on the safe properties:

$$R_{CBF}(\delta_t^P) = \begin{cases} r_n \cdot |a_{pt}(s_t)|, & \text{if } a_{pt}(s_t) \neq 0, \\ R'(\delta_t^P), & \text{if } a_{pt}(s_t) = 0, \end{cases} \quad (28)$$

where $r_n \in \mathbb{R}$ is a constant parameter s.t. $r_n < 0$.

- (2) The automaton component \bar{q}_{t+1} of product state x_{t+1} is updated:

$$\bar{q}_{t+1} = \begin{cases} \bar{q} \text{ s.t. } \bar{q} \in \bar{Q}_{unsafe}, & \text{if } a_{pt}(s_t) \neq 0 \\ \bar{\delta}(\bar{q}_t, L(s_t)), & \text{if } a_{pt}(s_t) = 0. \end{cases} \quad (29)$$

- (3) Instead of storing information $a_{Safe}(s_t)$, $R'(\delta_t^P)$, add

$(x_t, a_{RL}(s_t), R_{CBF}(\delta_t^P), x_{t+1})$ to replay buffer for training.

In the (28), $r_n < 0$ s.t. $r_n \cdot |a_{pt}(s_t)|$ represents how much the $a_{RL}(s_t)$ violates the safe constraint $\square\phi_{safe}$, which is proportional to the absolute value of CBF compensators. Similarly, the (29) switches the obtained automaton state \bar{q}_{t+1} to be the state of \bar{Q}_{unsafe} in Def. 9. Different from the work [14] that takes $a_{Safe}(s_t)$ into the replay buffer for training, third step keeps the original modular RL controller $a_{RL}(s_t)$ integrating with the shaped reward R_{CBF} into training. As for actor-critic methods of the modular RL, such a design can improve the efficiency of exploration and stabilize the learning results, since the controllers a_{RL} in relay buffer are generated from the policy distributions of the actor, whereas controllers a_{Safe} are only for safe execution that are not consistent with the outputs of the modular actor-critic architecture. The overall procedure of safe learning and guiding is illustrate in Line (7-12) of Alg. 1. This idea of enforcing optimal policies is illustrated in Fig. 3 (b). Finally, we show that the original optimal policies generating from Section IV remain invariant applying safe learning and guiding processes.

Theorem 6. Given a cl-MDP \mathcal{M} and an E-LDGBA $\bar{\mathcal{A}}_\phi$, the optimal policy π^* generated by combining the modular DDPG and three-step exploration guiding procedure in Def. 17 maximizes the probability of satisfying ϕ in the limit.

Proof. The safe guiding is to efficiently enhance the $a_{pt}(s_t)$ rapidly decaying to 0. Based on Def. 17, the intuitive of safe guiding is to bridge the connection between the unsafe component \bar{Q}_{unsafe} of E-LDGBA and ECBF controllers $a_{pt}(s_t)$ s.t. $a_{pt}(s_t) \neq 0$ indicates the original $a_{RL}(s_t)$ violates the safe requirement of $\phi = \square\phi_{safe} \wedge \phi_g$. Consequently, the objective is to verify that assigning negative reward to the states x with automaton components $q \in \bar{Q}_{unsafe}$ preserves optimal solutions in Proposition 1 and Theorem 4. We show the proof by contradiction. See appendix A-E for more details. \square

Safe guiding integrates the property of violation for the LTL formula $\phi = \square\phi_{safe} \wedge \phi_g$ and the safe set to enforce the efficient exploration. Then $a_{pt}(s_t)$ gradually decays to 0 and becomes inactive. The overall structure pushes the RL policies generated from the set of safe polices without altering the original optimality, while maintaining safe during learning.

VI. EXPERIMENTS

We demonstrate the framework in several environments with corresponding LTL tasks. To show the effectiveness of safe modular DDPG with guiding enabled, we compare our framework referred as safe modular with guiding (Modular-DDPG-ECBF-Guiding) with three baselines: (i) safe standard DDPG with guiding (Standard-DDPG-ECBF-Guiding), (ii) modular or standard DDPG without safe module enabled (Standard-DDPG, Modular-DDPG), (iii) safe modular DDPG without guiding (Modular-DDPG-ECBF-off-Guiding). We therefore consider four variants of the baselines as summarized in Table I. A tool Owl [45] is used to convert LTL specifications to LDGBA that are then manually transformed into E-LDGBA. Various implementations based on OpenAI gym are carried out

TABLE I
BASELINE VARIANTS TESTED IN CASE STUDY.

Baseline	Modular DDPG	Standard DDPG	Safe Module	Exploration Guiding
Modular-DDPG-ECBF-(On)-Guiding	✓	X	✓	✓
Modular-DDPG-ECBF-Off-Guiding	✓	X	✓	X
Modular-DDPG	✓	X	X	X
Standard-DDPG	X	✓	X	X

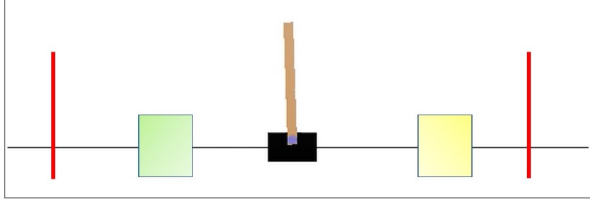


Fig. 5. Demonstration of LTL tasks for Cart-Pole.

on a machine with 3.60 GHz quad-core CPU, 16 GB RAM, an external Nvidia RTX 1080 GPU and Cuda enabled. The details of experimental setting can be found in Appendix A-F.

It's worth to point out that it's more challenging for RL agent satisfying tasks over infinite horizons. Consequently, We focus on the evaluation of the infinite-horizon formulas and analyze their success rates of the formulas at the end (Fig. 16). The safe sets and control barrier functions are defined separately for each dynamic system, and Fig. 15 shows the safety rates of all tasks through different baselines. The video demonstrations can be found in our YouTube channel ¹.

A. Cart-Pole and Inverted-Pendulum

We first apply algorithms to the control of simulated environments powered by the OpenAI gym. The LTL formulas over infinite horizons are all formulated as the form $\phi_{g_1} = \square \Diamond R_{\text{green}} \wedge \square \Diamond R_{\text{yellow}}$, which require to visit the blue and green regions infinitely often, while staying within the safe set ϕ_{safe} . And the tasks over finite horizons are in the form of $\phi_{g_2} = \Diamond (R_{\text{green}} \wedge \Diamond R_{\text{yellow}})$.

Cart-Pole: The physical simulation of Cart-Pole is introduced in Fig. 5. In this case, a pendulum is attached to a cart that moves horizontally along a friction-less track, and the control input is a horizontal force to the cart. Denote $s = [\theta_p, s_c, \dot{\theta}_p, \dot{s}_c]^T$ as the state (cart position, pendulum angle and corresponding velocities) of the dynamic system and its true dynamics are defined as follows:

$$\ddot{\theta}_p = \frac{(u - d) + h_1 \cos \theta_p \sin \theta_p + h_2 \dot{\theta}_p^2 \sin \theta_p}{h_3 + h_4 \cos^2 \theta_p},$$

$$\ddot{s}_c = \frac{g_1(u - d) \cos \theta_p + g_2 \dot{\theta}_p^2 \cos \theta_p \sin \theta_p + g_3 \sin \theta_p}{g_4 + g_5 \cos^2 \theta_p},$$

where external control force limit $a \in [-20N, 20N]$, and h_1, \dots, h_4 and g_1, \dots, g_4 are the physic parameters. To introduced model uncertainty, one assumes 30% error in the

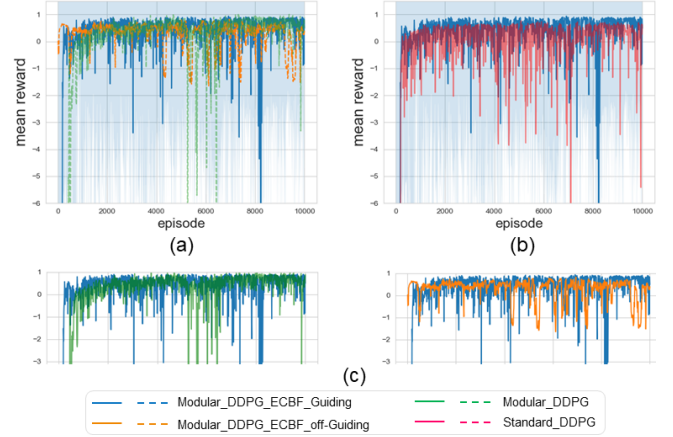


Fig. 6. Cart-Pole: Average training rewards of the LTL formula ϕ_{Cart1} . (a) The results of baselines: Modular DDPG, safe modular with guiding, safe modular without guiding. (b) The comparison between safe modular and standard DDPG. (c) Extraction of the results in (a) for detailed comparison.

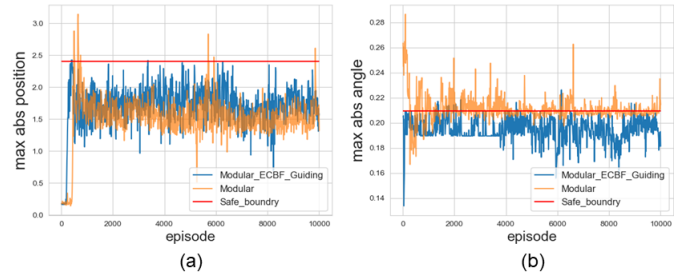


Fig. 7. Cart-Pole: Maximum absolute value of position (a) and angles (b) of the LTL formula ϕ_{Cart1} for baselines modular DDPG and safe modular DDPG during training.

physic constants. The safe set of two control barrier functions is introduced as

$$\mathcal{C}_1 = \{(\theta_p, s_c) : (12^2 - \theta_p^2 \geq 0) \wedge (2.4^2 - s_c^2 \geq 0)\}.$$

The corresponding LTL formula that hold the system stay at safe set \mathcal{C}_1 for current state is defined as $\phi_{\text{safe}} = \phi_{\mathcal{C}_1}$. The overall LTL formula over infinite horizons can be $\phi_{\text{Cart1}} = \square \phi_{\mathcal{C}_1} \wedge \phi_{g_1}$, where ϕ_{g_1} requires the agent to periodically visit blue and green regions that are located range from -1.44 to -0.96 m and from 0.96 to 1.44 m, respectively, and the LTL formula over finite horizons can be $\phi_{\text{Cart2}} = \square \phi_{\mathcal{C}_1} \wedge \phi_{g_2}$, where ϕ_{g_2} requires the agent to sequentially visit blue and green regions. The results of ϕ_{Cart1} are shown in Fig. 6, 7, 8.

Fig.6 compares the mean reward achieved via different baselines. Fig.6 (c) extracts the results of Fig.6 (a) for more detailed comparison. Fig.6 (a) and (c) show that safe modular DDPG and modular DDPG achieve the same performance

¹<https://www.youtube.com/watch?v=gXSS-EQ9Scc>

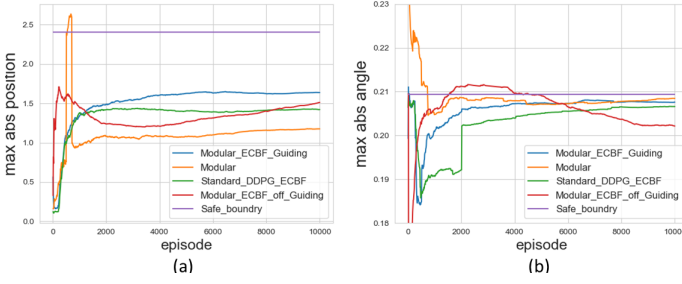


Fig. 8. Cart-Pole: Maximum absolute value of positions (a) and angles (b) of the LTL formula ϕ_{Cart1} for different baselines during evaluation process.

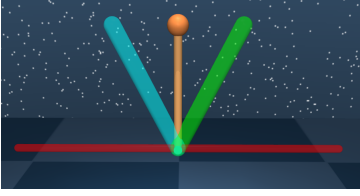


Fig. 9. Demonstration of LTL Task for Inverted-Pendulum.

of task satisfaction such that the safe module with guiding will maintain safe during training and will not alter the RL optimality, and the safe modular without guiding will influence the exploration and RL optimality. Fig.6 (b) states the modular DDPG has better performance than the standard DDPG (higher rewards). Even though there's a slightly higher rewards using modular architecture in Fig.6 (b), it will influence the success rates of optimal policies completing the task over infinite horizons as shown in Fig. 16.

Fig.7 and Fig.8 show the absolute value of maximum angle and position of each episode during learning and evaluation process, respectively. First, Fig.7 demonstrates the benefits of applying the safe module such that the ECBF compensators as minimal perturbations safeguard the RL-agent during learning. Then Fig.8 compares the safe performance using different baselines. Especially, it shows the advantage of the guiding procedure. Since the dynamics of Cart-Pole is more complex and sensitive and the RL controllers always render the systems to be operating around the margin of the safe set, which makes the safety easier to be violated when the exploration guiding is not enabled. The safety rates of infinite-horizons task ϕ_{Cart1} and finite-horizons task ϕ_{Cart2} using different baselines are shown in Fig. 15, which illustrates the improvement of the exploration guiding.

Inverted-Pendulum: The physical simulation of inverted-pendulum is introduced in Fig. 9. The true dynamic of state θ that has mass m , length l and torque u is introduced as follows:

$$\dot{\theta} = \frac{3g}{2l} \sin \theta + \frac{3}{2ml^2} u,$$

where torque limit is $[-15, 15]$ and nominal model assumes to have 40% errors of parameters. The safe set of a control barrier function is defined $C_2 = \{\theta : (\frac{\pi^2}{2} \geq 0)\}$. The corresponding LTL formula that hold the system stay at safe set C_2 is defined as $\phi_{\text{safe}} = \phi_{C_2}$. The whole LTL formula over infinite horizons can be $\phi_{\text{Pen1}} = \Box \phi_{C_2} \wedge \phi_{g_{P1}}$, where $\phi_{g_{P1}}$ requires the agent to

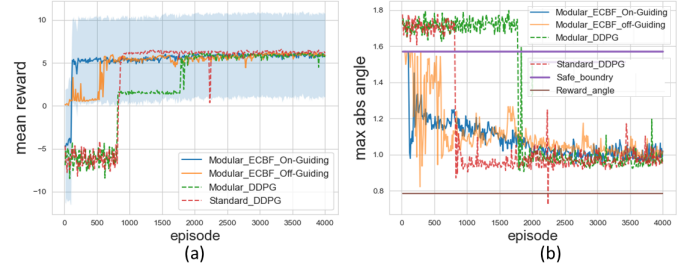


Fig. 10. Inverted-Pendulum: reward collections and maximum absolute angles of the formula ϕ_{Pen1} . (a) Mean reward. (b) Maximum absolute angles

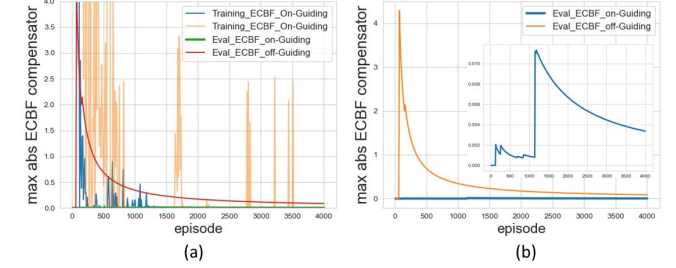


Fig. 11. Inverted-Pendulum: comparison of the formula ϕ_{Pen1} between the algorithms with and without safe guiding enabled. (left) Maximum absolute value of ECBF compensators during learning. (right) Magnified ECBF compensators during evaluation.

periodically visit blue and green regions that are located at $-\frac{\pi}{4}$ rads and $\frac{\pi}{4}$ rads, respectively, and the LTL formula over finite horizons can be $\phi_{\text{Pen2}} = \Box \phi_{C_2} \wedge \phi_{g_{P2}}$, where $\phi_{g_{P2}}$ requires the agent to sequentially visit blue and green regions. The analysis of ϕ_{Pen1} is shown in Fig. 10 and 11.

Fig.10 (a) (b) compares the mean reward and absolute value of maximum angles during learning process generated via different baselines, respectively. Especially, Fig.10 (a) shows that the safe modular learning with exploration guiding can be more efficient to find the optimal policies, since the guiding module will enforce the exploration within a set of safe policies. In addition, Fig.10 (b) shows the importance of the safe module during learning process. At the same time, Fig. 11 focuses on illustrating the effectiveness of the exploration guiding and compares the baselines during learning and evaluation process. By assigning negative rewards when the ECBF controllers involved, it's shown that the our algorithm enhances the RL-agent updating within the safe set and leads the output of ECBF compensators to dramatically decay.

B. Particle Gym and Mars Rover

We test the algorithms to the control of a car-like model. Let $s = [p_x, p_y, \theta, v]^T$, $a = [u, \phi]^T$, and L denote the state (position, heading, velocity), control variables (acceleration, steering angle), and length of the vehicle, respectively. The dynamics of the model are as follows:

$$\dot{s} = [v \cos \theta, v \sin \theta, \frac{\tan \phi}{L}, K_u u]^T$$

where K_u is the physical constant. To model the unknown model, we set 25% error in the parameters L and K_u and add Gaussian noise to the accelerations.

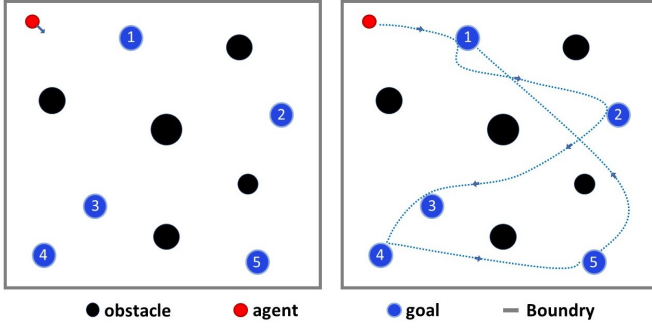


Fig. 12. Image left is the initial state of the system, where red circle represents the mobile robot, and other colored circles represent the goals and obstacles. In addition, the RL-agent is also required to move within the rectangular box. Image right is the simulated trajectory for the task φ_{Gym_1} with a repetitive pattern.

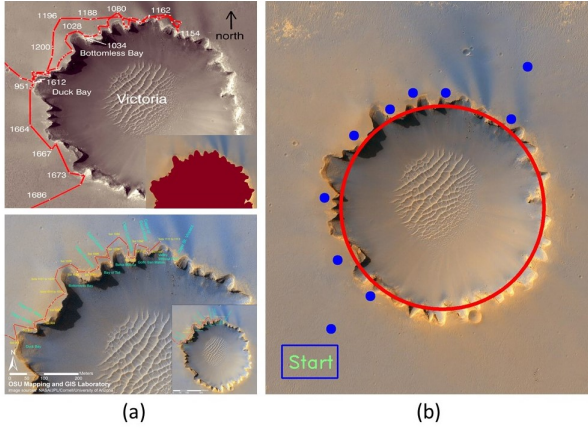


Fig. 13. Demonstration of LTL Task for Victoria Crater Mars Exploration.

Particle Gym: We first test our algorithm in the particle gym environment as shown in Fig. 12. The two missions of RL-agent (red circle) require to sequentially visit the blue regions from number 1 to 5 over infinite and finite horizons, respectively. The safety is to always avoid the black obstacles and stay within the rectangular workspace, which can be encoded as multiple decentralized ECBFs. The LTL task over infinite horizons can be formulated as:

$$\phi_{Gym_1} = \Box((\Diamond R_1 \wedge \Diamond(R_2 \wedge \Diamond \dots \wedge R_5)) \rightarrow R_1) \wedge \Box \phi_{C_3},$$

where R_i is i -th blue region indexed with a number i , and ϕ_{C_3} represents safety requirements associated with ECBFs. The simulated trajectory of φ_{Gym_1} for one round of the repetitive satisfaction is shown in Fig. 12 (b). Also the task over finite horizons version can be $\phi_{Gym_2} = (\Diamond R_1 \wedge \Diamond(R_2 \wedge \Diamond \dots \wedge R_5)) \rightarrow R_1 \wedge \Box \phi_{C_3}$. The results of mean reward collection for the task φ_{Gym_1} during training compared with two baselines are shown in Fig. 14 (left), which illustrates the better performance of modular architecture and effectiveness of the exploration guiding.

Mars Rover: We then implement our algorithm in a large scale and pixel-based environment, and conduct motion planning to complete complex exploration missions using satellite images as shown in Fig. 13. The missions are to

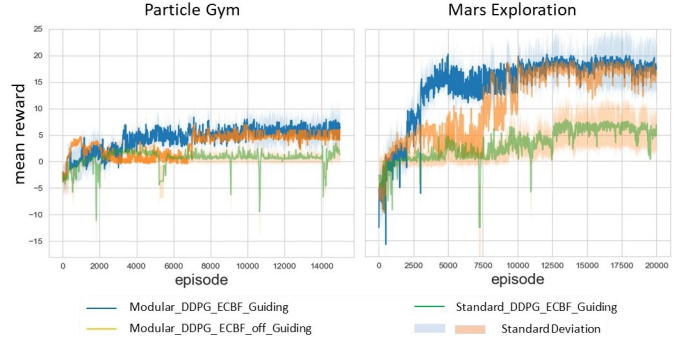


Fig. 14. Mean reward collection during training for particle gym (left) and Mars exploration (right). We analyze the results of tasks φ_{Gym_1} and φ_{V_1} over infinite horizons to demonstrate the effectiveness and efficiency of the modular architecture and safe learning process.

explore areas around the Victoria Crater [55] shown in Fig. 13 (a), which is an impact crater located near the equator of Mars. Layered sedimentary rocks are exposed along the wall of crater, providing information about the ancient surface condition of Mars. The mission is related to visiting all spots along with the path of the well-known Mars Rover Opportunity, which is shown in Fig. 13 (b), and avoiding the unsafe areas (red circle). The LTL specification specifying such missions over infinite horizons is expressed as:

$$\phi_{V_1} = \Box((\Diamond V_1 \wedge \Diamond(V_2 \wedge \Diamond \dots \wedge V_{10})) \rightarrow V_{Start}) \wedge \Box \phi_{C_4},$$

where V_i denotes i -th target (blue spot) counts from bottom-left to top-right. ϕ_{C_4} represents safety requirements (barrier functions) s.t. the agent should always avoid the unsafe crater area marked as red circle in Fig. 13 (b). The description of overall task in English is "visit the target from 1 to 10 and then return to the start position, repetitively, while avoiding the unsafe regions". Similarly, the corresponding task over finite horizons version can be $\phi_{V_2} = (\Diamond V_1 \wedge \Diamond(V_2 \wedge \Diamond \dots \wedge V_{10})) \rightarrow V_{Start} \wedge \Box \phi_{C_4}$. The results of mean reward collection for the task φ_{Gym_1} during training compared with two baselines are shown in Fig. 14 (right), which also shows the better performance and effectiveness of safe modular DDPG with guiding enabled.

C. Complexity and Performance Analysis

First, safety rates is the number of safe episodes versus all episodes, and Fig. 15 shows the safety rates for all tasks over all environments through different baselines. It shows that the benefits of the ECBF-based safe module and the improvement of the exploration guiding. Then, we analyze the training complexity for various baselines shown in Table II. From the aspect of safe learning, the developed safe module requires to solve quadratic programming at each step, and the training time increased for both safe modular and safe standard DDPG methods. This is reasonable since the algorithm needs to check whether controllers are safe at each step. As for the aspect of modular architecture, even though it adopts several distributed actor-critic neural network pairs, they are synchronously trained online, and each of them is only responsible for a sub-task. Consequently, the training time will mainly be influenced by the number of steps and episodes for both safe modular and

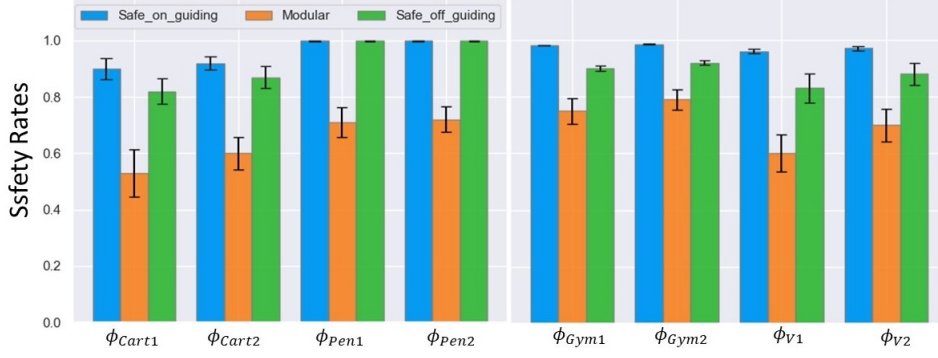


Fig. 15. Safety rates analysis for each environments that includes corresponding infinite-horizons and finite-horizons tasks. The results are all conducted using modular RL algorithm and enabling different modules, and are taken over 10 independent learning trials.

TABLE II
TRAINING TIME ANALYSIS OF ALGORITHMS WITH AND WITHOUT SAFE MODULE (ECBF-BASED CONTROL AND EXPLORATION GUIDING).

Tasks and Training Parameters			Training Time (hour)			
LTL Task	Maximum steps	Episode	Modular DDPG	Safe Modular DDPG	Standard DDPG	Safe Standard DDPG
φ_{B1}	300	10000	5.5	7.2	5.0	7.1
φ_{B2}	300	10000	4.9	6.3	4.6	6.3
φ_{C1}	200	4000	3.6	4.0	3.5	4.0
φ_{C2}	200	4000	2.0	2.5	2.1	2.8
φ_{Gym1}	1000	15000	9.7	11.9	9.3	12.1
φ_{Gym2}	1000	15000	7.3	10.5	8.5	12.0
φ_{V1}	5000	20000	22.7	40.4	26.9	41.6
φ_{V2}	5000	20000	14.3	18.2	21.0	28.5

standard DDPG. For the complex tasks e.g. φ_{V2} , the modular architecture can complete the task faster (terminate the episode earlier) during learning, and reduce the training time.

To state the performance of the modular structure, we mainly compare the methods safe modular DDPG and safe standard DDPG that are both enabled with exploration guiding. Then, we take 200 runs applying the learned model, and analyze the success rate for all aforementioned tasks. Due to growing dimensions of automaton structure for more complex tasks and limited training process in practice, it becomes more difficult for standard DDPG to explore the whole tasks over infinite horizons, and distinguish the procedure of the satisfaction. As shown in Fig. 16, we can conclude that modular architecture has better and more stable performance, whereas the standard DDPG yields poor performance for complex tasks with repetitive pattern (infinite horizons).

VII. CONCLUSIONS

Achievement of safe critical requirements during learning is a challenging problem with a significant real-world applicability. Part of the challenge stems from the uncertain and unknown dynamic systems, and the impact of the exploration involving optimal solutions. Such a problem becomes even more difficult but more meaningful when RL-agents are tasked to accomplish complex human instructions over infinite horizons and continuous space. The main difficulties are due to the nature of nonlinear regression to recognize each stage of task-satisfaction and the need for large training episodes. Therefore, we propose the ECBF-based safe RL framework combining with GPs for estimation of the nominal systems, and train an

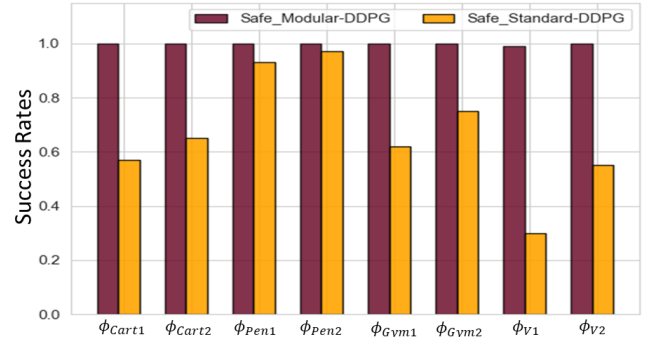


Fig. 16. Performance evaluation through success rates for all tasks respectively. Every evaluation is conducted with the same steps in Table II.

RL agent guided by the LTL specifications to describe high-level complex tasks. These features will be crucial in employing reinforcement learning on physical applications, where human are able to formulate advanced objectives specified in the formal language. They are also important in the case where problems require online efficient computation and effective learning performance.

This frameworks combines model-free deep RL, GP-based ECBF control and automata theory of compositional LTL syntax. On the training side, the designed E-LDGBA allows us to apply the deterministic policy and overcome the issue of sparse rewards, and the reward shaping technique further enhance dense rewards. On the evaluation side, by fully utilizing the automaton structure, we synthesis a innovative modular DDPG architecture that relies on the distributed

neural networks to improve the performance of the learning results for complex tasks. We also propose a novel approach by integrating the sink components of LTL automaton and ECBF perturbations to enforce the guiding of exploration. A significant formal verification is that the above modules (safe and modular) will not have impact to desired behaviors with respect to original optimal solutions i.e., satisfying LTL with maximum probability in the limit.

We implement the overall algorithm in various control systems and demonstrate its benefits by comparing with several baselines. Our results are encouraging for several future directions. This work assumes we are given a valid safe set of ECBF that can be rendered forward invariant, which opens the questions of whether we can learn the ECBF in addition to the controllers. Future lines will also consider multi-agent cooperative tasks and safe learning that are scalable on the number of agents.

VIII. ACKNOWLEDGEMENTS

The authors would like to thank Mohammadhosein Hasanbeig for previous efforts [37]. The authors also thank Richard Cheng for discussions regarding CBFs.

APPENDIX A RELEVANT PROOF

A. Proof of Lemma 1

We prove (1) by showing that $\mathcal{L}(\bar{\mathcal{A}}_\phi) \supseteq \mathcal{L}(\mathcal{A}_\phi)$ and $\mathcal{L}(\bar{\mathcal{A}}_\phi) \subseteq \mathcal{L}(\mathcal{A}_\phi)$.

Case 1: $\mathcal{L}(\bar{\mathcal{A}}_\phi) \supseteq \mathcal{L}(\mathcal{A}_\phi)$: For any accepting language $\omega = \alpha_0\alpha_1 \dots \in \mathcal{L}(\mathcal{A}_\phi)$, there exists a corresponding run $\mathbf{r} = q_0\alpha_0q_1\alpha_1 \dots$ of \mathcal{A}_ϕ s.t.

$$\inf(\mathbf{r}) \cap F_i \neq \emptyset, \forall i \in \{1, \dots, f\}. \quad (30)$$

For the run \mathbf{r} , we can construct a sequence $\bar{\mathbf{r}} = \bar{q}_0\alpha_0\bar{q}_1\alpha_1 \dots$ by add each state q with the set T , which is synchronously updated via (4) after each transition. It can be verified that such a run $\bar{\mathbf{r}}$ is a valid run of $\bar{\mathcal{A}}_\phi$ based on Def. 7. According to (30), since the tracking-frontier set T will be reset once all accepting sets have been visited, it holds $\inf(\bar{\mathbf{r}}) \cap \bar{F}_i \neq \emptyset, \forall i \in \{1, \dots, f\}$ s.t. $\omega \in \mathcal{L}(\bar{\mathcal{A}}_\phi)$.

Case 2: $\mathcal{L}(\bar{\mathcal{A}}_\phi) \subseteq \mathcal{L}(\mathcal{A}_\phi)$: Similarly, for any accepting language $\bar{\omega} = \bar{\alpha}_0\bar{\alpha}_1 \dots \in \mathcal{L}(\bar{\mathcal{A}}_\phi)$, there exists a corresponding run $\bar{\mathbf{r}} = \bar{q}_0\bar{\alpha}_0\bar{q}_1\bar{\alpha}_1 \dots$ of $\bar{\mathcal{A}}_\phi$ s.t.

$$\inf(\bar{\mathbf{r}}) \cap \bar{F}_i \neq \emptyset, \forall i \in \{1, \dots, f\}. \quad (31)$$

For the run $\bar{\mathbf{r}}$, we can construct a sequence $\mathbf{r} = q_0\bar{\alpha}_0q_1\bar{\alpha}_1 \dots$ by projecting each state $\bar{q} = (q, T)$ into q . It can be simply verified that such a run \mathbf{r} is a valid run of \mathcal{A}_ϕ based on Def. 7. According to (31), it holds $\inf(\mathbf{r}) \cap F_i \neq \emptyset, \forall i \in \{1, \dots, f\}$ s.t. $\bar{\omega} \in \mathcal{L}(\mathcal{A}_\phi)$.

B. Proof of Lemma 2

The strategy of the following proof is based on contradiction. Assume there exists a policy such that $R_\pi^j \cap F_k^P \neq \emptyset, \forall k \in K$, where K is a subset of $2^{\{1, \dots, f\}} \setminus \{\{1, \dots, f\}, \emptyset\}$. As discussed in [46], for each state in recurrent class, it holds

that $\sum_{n=0}^{\infty} p^n(x, x) = \infty$, where $x \in R_\pi^j \cap F_k^P$ and $p^n(x, x)$ denotes the probability of returning from a transient state x to itself in n steps. This means that each state in the recurrent class occurs infinitely often. However, based on the embedded tracking-frontier function of EP-MDP, once x_k is visited, the corresponding F_k of F_k^P is removed from T , and the tracking set T will not be reset until all accepting sets have been visited. As a result, neither $q_k \in F_k$ nor $x_k = (s, q_k, T) \in R_\pi^j \cap F_k^P$ with $s \in S$ will occur infinitely, which contradicts the property $\sum_{n=0}^{\infty} p^n(x_k, x_k) = \infty$.

C. Proof of Theorem 1

Lemma 5. For any path \mathbf{x}_t and $\mathcal{D}(\mathbf{x}_t)$ in (8), it holds that $0 \leq \gamma_F \cdot \mathcal{D}(\mathbf{x}_t[t+1:]) \leq \mathcal{D}(\mathbf{x}_t) \leq 1 - r_F + r_F \cdot \mathcal{D}(\mathbf{x}_t[t+1:]) \leq 1$, where $\mathbf{x}_t[t+1:]$ denotes the suffix of \mathbf{x}_t starting from x_{t+1} . Let $BSCC(MC_\pi^P)$ denote the set of all BSCCs of an induced Markov chain MC_π^P and let X_π^P denotes the set of accepting states that belongs to a BSCC of MC_π^P s.t. $X_\pi^P := \{x \in X \mid x \in F_U^P \cap BSCC(MC_\pi^P)\}$. Then, for any states $x \in X_\pi^P$, it holds that $\lim_{\gamma_F \rightarrow 1^-} U^\pi(x) = 1$.

The proof of Lemma 5 is omitted since it is a straightforward extension of Lemma 2 and Lemma 3 in [32], by replacing LDBA with E-LDGBA.

Based on whether or not the path \mathbf{x}_t intersects with accepting states of F_i^P , the expected return in (9) can be rewritten as

$$U^\pi(x) = \mathbb{E}^\pi[\mathcal{D}(\mathbf{x}_t) \mid \mathbf{x}_t \models \Diamond F_i^P] \cdot \Pr^\pi[x \models \Diamond F_i^P] + \mathbb{E}^\pi[\mathcal{D}(\mathbf{x}_t) \mid \mathbf{x}_t \not\models \Diamond F_i^P] \cdot \Pr^\pi[x \not\models \Diamond F_i^P] \quad (32)$$

where $\Pr^\pi[x \models \Diamond F_i^P]$ and $\Pr^\pi[x \not\models \Diamond F_i^P]$ represent the probability of eventually reaching and not reaching F_i^P eventually under policy π starting from state x , respectively.

To find the lower bound of $U^\pi(x)$, for any \mathbf{x}_t with $\mathbf{x}_t[t] = x$, let $t + N_t$ be the index that \mathbf{x}_t first intersects a state in X_π^P , i.e., $N_t = \min[i \mid \mathbf{x}_t[t+i] \in X_\pi^P]$. The following holds

$$\begin{aligned} & \mathbb{E}^\pi[\mathcal{D}(\mathbf{x}_t) \mid \mathbf{x}_t \models \Diamond F_i^P] \\ & \stackrel{(1)}{\geq} \mathbb{E}^\pi[\mathcal{D}(\mathbf{x}_t) \mid \mathbf{x}_t \cap X_\pi^P \neq \emptyset] \\ & \stackrel{(2)}{\geq} \mathbb{E}^\pi[\gamma_F^{N_t} \cdot \mathcal{D}(\mathbf{x}_t[t+N_t:]) \mid \mathbf{x}_t[t+N_t] = x \mid \mathbf{x}_t \cap X_\pi^P \neq \emptyset] \\ & \stackrel{(3)}{\geq} \mathbb{E}^\pi[\gamma_F^{N_t} \mid \mathbf{x}_t \cap X_\pi^P \neq \emptyset] \cdot U_{\min}^\pi(\mathbf{x}_t[t+N_t]) \\ & \stackrel{(4)}{\geq} \gamma_F^{\mathbb{E}^\pi[N_t \mid \mathbf{x}_t[t]=x \mid \mathbf{x}_t \cap X_\pi^P \neq \emptyset]} \cdot U_{\min}^\pi(x_{Acc}) \\ & = \gamma_F^{n_t} \cdot U_{\min}^\pi(x_{Acc}), \end{aligned} \quad (33)$$

where $x_{Acc} \in X_\pi^P$, $U_{\min}^\pi(x_{Acc}) = \min_{x \in X_\pi^P} U^\pi(x)$, and n_t is a constant. By Lemma 5, one has $\lim_{\gamma_F \rightarrow 1^-} U_{\min}^\pi(x_{Acc}) = 1$.

In (33), the first inequality (1) holds because visiting X_π^P is one of the cases for $\Diamond F_i^P$ that satisfy $\mathbf{x}_t \models \Diamond F_i^P$, e.g., F_i^P can be placed outside of all BSCCs; the second inequality (2) holds due to Lemma 5; the third inequality (3) holds due to the Markov properties of (8) and (9); the fourth inequality (4) holds due to Jensen's inequality. Based on (33), the lower

bound of (32) is $U^\pi(x) \geq \gamma_F^{n_t} \cdot U_{\min}^\pi(x_{Acc}) \cdot \Pr^\pi[x \models \Diamond F_i^{\mathcal{P}}]$ from which one has

$$\lim_{\gamma_F \rightarrow 1^-} U^\pi(x) \geq \gamma_F^{n_t} \cdot \Pr^\pi[x \models \Diamond F_i^{\mathcal{P}}]. \quad (34)$$

Similarly, let $t + M_t$ denote the index that x_t first enters the BSCC that contains no accepting states. We have

$$\begin{aligned} \mathbb{E}^\pi[\mathcal{D}(x_t) | x_t \not\models \Diamond F_i^{\mathcal{P}}] &\stackrel{(1)}{\leq} \mathbb{E}^\pi[1 - r_F^{M_t} | x_t \not\models \Diamond F_i^{\mathcal{P}}] \\ &\stackrel{(2)}{\leq} 1 - r_F^{\mathbb{E}^\pi[M_t | x_t[t]=x, x_t \not\models \Diamond F_i^{\mathcal{P}}]} = 1 - r_F^{m_t} \end{aligned} \quad (35)$$

where m_t is a constant and (35) holds due to Lemma 5 and Markov properties.

Hence, the upper bound of (32) is obtained as

$$\lim_{\gamma_F \rightarrow 1^-} U^\pi(x) \leq \Pr^\pi[x \models \Diamond F_i^{\mathcal{P}}] + (1 - r_F^{m_t}) \Pr^\pi[x \not\models \Diamond F_i^{\mathcal{P}}]. \quad (36)$$

By (34) and (36), we can conclude

$$\begin{aligned} \gamma_F^{n_t} \cdot \Pr^\pi[x \models \Diamond F_i^{\mathcal{P}}] &\leq \lim_{\gamma_F \rightarrow 1^-} U^\pi(x) \\ &\leq \Pr^\pi[x \models \Diamond F_i^{\mathcal{P}}] + (1 - r_F^{m_t}) \cdot \Pr^\pi[x \not\models \Diamond F_i^{\mathcal{P}}] \end{aligned}$$

According to $\lim_{\gamma_F \rightarrow 1^-} r_F(\gamma_F) = 1$ in the reward function, (10) can be concluded.

D. Proof of Theorem 2

For any policy π , $MC_\pi^\pi = \mathcal{T}_\pi \sqcup \mathcal{R}_\pi^1 \sqcup \mathcal{R}_\pi^2 \dots \mathcal{R}_\pi^{n_R}$. Let $U_\pi = [U^\pi(x_0) \ U^\pi(x_1) \ \dots]^T \in \mathbb{R}^{|X|}$ denote the stacked expected return under policy π , which can be reorganized as

$$\begin{aligned} \begin{bmatrix} U_\pi^{tr} \\ U_\pi^{rec} \end{bmatrix} &= \sum_{n=0}^{\infty} \left(\prod_{j=0}^{n-1} \begin{bmatrix} \gamma_\pi^T & \gamma_\pi^{tr} \\ \mathbf{0}_{\sum_{i=1}^m N_i \times r} & \gamma_\pi^{rec} \end{bmatrix} \right) \\ &\quad \cdot \begin{bmatrix} P_\pi(\mathcal{T}, \mathcal{T}) & P_\pi^{tr} \\ \mathbf{0}_{\sum_{i=1}^m N_i \times r} & P_\pi(\mathcal{R}, \mathcal{R}) \end{bmatrix}^n \begin{bmatrix} R_\pi^{tr} \\ R_\pi^{rec} \end{bmatrix}, \end{aligned} \quad (37)$$

where U_π^{tr} and U_π^{rec} are the expected return of states in transient and recurrent classes under policy π , respectively. In (37), $P_\pi(\mathcal{T}, \mathcal{T}) \in \mathbb{R}^{r \times r}$ is the probability transition matrix between states in \mathcal{T}_π , and $P_\pi^{tr} = [P_\pi^{tr_1} \dots P_\pi^{tr_m}] \in \mathbb{R}^{r \times \sum_{i=1}^m N_i}$ is the probability transition matrix where $P_\pi^{tr_i} \in \mathbb{R}^{r \times N_i}$ represents the transition probability from a transient state in \mathcal{T}_π to a state of \mathcal{R}_π^i . The $P_\pi(\mathcal{R}, \mathcal{R})$ is a diagonal block matrix, where the i th block is a $N_i \times N_i$ matrix containing transition probabilities between states within \mathcal{R}_π^i . Note that $P_\pi(\mathcal{R}, \mathcal{R})$ is a stochastic matrix since each block matrix is a stochastic matrix [46]. Similarly, the rewards R_π can also be partitioned into R_π^{tr} and R_π^{rec} .

The following proof is based on contradictions. Suppose there exists a policy π^* that optimizes the expected return, but does not satisfy the accepting condition of \mathcal{P} with non-zero probability. Based on Lemma 2, the following is true: $F_k^{\mathcal{P}} \subseteq \mathcal{T}_{\pi^*}, \forall k \in \{1, \dots, f\}$, where \mathcal{T}_{π^*} denotes the transient class of Markov chain induced by π^* on \mathcal{P} . First, consider a state $x_R \in \mathcal{R}_{\pi^*}^j$ and let $P_{\pi^*}^{x_R R_j}$ denote a row vector of $P_{\pi^*}^n(\mathcal{R}, \mathcal{R})$ that contains the transition probabilities from x_R

to the states in the same recurrent class $\mathcal{R}_{\pi^*}^j$ after n steps. The expected return of x_R under π^* is then obtained from (37) as

$$U_{\pi^*}^{rec}(x_R) = \sum_{n=0}^{\infty} \gamma^n \left[\mathbf{0}_{k_1}^T P_{\pi^*}^{x_R R_j} \mathbf{0}_{k_2}^T \right] R_{\pi^*}^{rec},$$

where $k_1 = \sum_{i=1}^{j-1} N_i$, $k_2 = \sum_{i=j+1}^n N_i$. Since $\mathcal{R}_{\pi^*}^j \cap F_i^{\mathcal{P}} = \emptyset, \forall i \in \{1, \dots, f\}$, by the designed reward function, all entries of $R_{\pi^*}^{rec}$ are zero. We can conclude $U_{\pi^*}^{rec}(x_R) = 0$. To show contradiction, the following analysis will show that $U_{\pi^*}^{rec}(x_R) > U_{\pi^*}^{rec}(x_R)$ for any policy $\bar{\pi}$ that satisfies the accepting condition of \mathcal{R} . Thus, it's true that there exists $\mathcal{R}_{\bar{\pi}}^j$ such that $\mathcal{R}_{\pi^*}^j \cap F_k^{\mathcal{P}} \neq \emptyset, \forall k \in \{1, \dots, f\}$. We use $\underline{\gamma}$ and $\bar{\gamma}$ to denote the lower and upper bound of γ .

Case 1: If $x_R \in \mathcal{R}_{\bar{\pi}}^j$, there exist states such that $x_A \in \mathcal{R}_{\bar{\pi}}^j \cap F_i^{\mathcal{P}}$. From Lemma 2, the entries in $R_{\bar{\pi}}^{rec}$ corresponding to the recurrent states in $\mathcal{R}_{\bar{\pi}}^j$ have non-negative rewards and at least there exist f states in $\mathcal{R}_{\bar{\pi}}^j$ from different accepting sets $F_i^{\mathcal{R}}$ with positive reward $1 - r_F$. From (37), $U_{\bar{\pi}}^{rec}(x_R)$ can be lower bounded as

$$U_{\bar{\pi}}^{rec}(x_R) \geq \sum_{n=0}^{\infty} \underline{\gamma}^n (P_{\bar{\pi}}^{x_R x_A} r_F) > 0, \quad (38)$$

where $P_{\bar{\pi}}^{x_R x_A}$ is the transition probability from x_R to x_A in n steps. We can conclude in this case $U_{\bar{\pi}}^{rec}(x_R) > U_{\pi^*}^{rec}(x_R)$.

Case 2: If $x_R \in \mathcal{T}_{\bar{\pi}}$, there are no states of any accepting set $F_i^{\mathcal{P}}$ in $\mathcal{T}_{\bar{\pi}}$. As demonstrated in [46], for a transient state $x_{tr} \in \mathcal{T}_{\bar{\pi}}$, there always exists an upper bound $\Delta < \infty$ such that $\sum_{n=0}^{\infty} p^n(x_{tr}, x_{tr}) < \Delta$, where $p^n(x_{tr}, x_{tr})$ denotes the probability of returning from a transient state x_T to itself in n time steps. In addition, for a recurrent state x_{rec} of $\mathcal{R}_{\bar{\pi}}^j$, it is always true that

$$\sum_{n=0}^{\infty} \gamma^n p^n(x_{rec}, x_{rec}) > \frac{1}{1 - \gamma^{\bar{n}} \bar{p}}, \quad (39)$$

where there exists \bar{n} such that $p^{\bar{n}}(x_{rec}, x_{rec})$ is nonzero and can be lower bounded by \bar{p} [46]. From (37), one has

$$\begin{aligned} U_{\bar{\pi}}^{tr} &> \sum_{n=0}^{\infty} \left(\prod_{j=0}^{n-1} \gamma_{\bar{\pi}}^{tr} \right) \cdot P_{\bar{\pi}}^{tr} P_{\bar{\pi}}^n(\mathcal{R}, \mathcal{R}) R_{\bar{\pi}}^{rec} \\ &> \underline{\gamma}^n \cdot P_{\bar{\pi}}^{tr} P_{\bar{\pi}}^n(\mathcal{R}, \mathcal{R}) R_{\bar{\pi}}^{rec}. \end{aligned} \quad (40)$$

Let $\max(\cdot)$ and $\min(\cdot)$ represent the maximum and minimum entry of an input vector, respectively. The upper bound $\bar{m} = \{\max(\bar{M}) | \bar{M} < P_{\bar{\pi}}^{tr} \bar{P} R_{\bar{\pi}}^{rec}\}$ and $\bar{m} \geq 0$, where \bar{P} is a block matrix whose nonzero entries are derived similarly to \bar{p} in (39). The utility $U_{\bar{\pi}}^{tr}(x_R)$ can be lower bounded from (39) and (40) as $U_{\bar{\pi}}^{tr}(x_R) > \frac{1}{1 - \gamma^{\bar{n}}} \bar{m}$. Since $U_{\pi^*}^{rec}(x_R) = 0$, the contradiction $U_{\bar{\pi}}^{tr}(x_R) > 0$ is achieved if $\frac{1}{1 - \gamma^{\bar{n}}} \bar{m}$. Thus, there exist $0 < \underline{\gamma} < 1$ such that $\gamma_F > \underline{\gamma}$ and $r_F > \underline{\gamma}$, which implies $U_{\bar{\pi}}^{tr}(x_R) > \frac{1}{1 - \gamma^{\bar{n}}} \bar{m} \geq 0$. The procedure shows the contradiction of the assumption that π^* that does not satisfy the acceptance condition of \mathcal{P} with non-zero probability is optimal, and Theorem 2 is proved.

E. Proof of Theorem 6

Suppose there exists a policy π^* that optimizes the expected return, but derives the system intersecting with \bar{Q}_{unsafe} with non-zero probability. Based on Lemma 2, the following is true: $F_k^P \subseteq \mathcal{T}_{\pi^*}, \forall k \in \{1, \dots, f\}$, where \mathcal{T}_{π^*} denotes the transient class of Markov chain induced by π^* on \mathcal{P} .

Consider two type of states $x_R \in \mathcal{R}_{\pi}^j$ and $x_T \in \mathcal{T}_{\pi}^j$. Let $\mathbf{P}_{\pi}^{x_R R_j}$ denote a row vector of $\mathbf{P}_{\pi}^n(\mathcal{R}, \mathcal{R})$ that contains the transition probabilities from x_R to the states in the same recurrent class \mathcal{R}_{π}^j after n steps. The expected return of x_R and x_T under π are then obtained from (37) respectively as

$$U_{\pi}^{rec}(x_R) = \sum_{n=0}^{\infty} \gamma^n \left[\mathbf{0}_{k_1}^T \mathbf{P}_{\pi}^{x_R R_j} \mathbf{0}_{k_2}^T \right] \mathbf{R}_{\pi}^{rec},$$

$$U_{\pi}^{tr} > \gamma^n \cdot \mathbf{P}_{\pi}^{tr} \mathbf{P}_{\pi}^n(\mathcal{R}, \mathcal{R}) \mathbf{R}_{\pi}^{rec},$$

where $k_1 = \sum_{i=1}^{j-1} N_i$, $k_2 = \sum_{i=j+1}^n N_i$, $\mathbf{P}_{\pi}^{tr} = [P_{\pi}^{tr_1} \dots P_{\pi}^{tr_m}] \in \mathbb{R}^{r \times \sum_{i=1}^m N_i}$ is the probability transition matrix, and the $\mathbf{P}_{\pi}(\mathcal{R}, \mathcal{R})$ is a diagonal block matrix.

Since $\mathcal{R}_{\pi^*}^j \cap \bar{X}_{unsafe} \neq \emptyset$ where \bar{X}_{unsafe} is introduced in Def. 14, all entries of $\mathbf{R}_{\pi^*}^{rec}$ are non-positive. We can conclude $U_{\pi^*}^{rec}(x_R) \leq 0$. To show contradiction, by selecting $\gamma_F \rightarrow 1^-$ the following analysis demonstrates the contradiction e.g., $U_{\pi}^{rec}(x_R) > U_{\pi^*}^{rec}(x_R)$, where π is a policy that satisfies the accepting condition of \mathcal{P} :

There exists two cases of the analysis. (i) $x_R \in \mathcal{R}_{\pi}^j$, we can obtain $U_{\pi}^{rec}(x_R) \geq 0$ from (38). (ii) $x_R \in \mathcal{T}_{\pi}$, the inequality $U_{\pi}^{tr}(x_R) > 0$ holds according to (39) and (40).

Accordingly, we prove the original optimal policies using based reward in Theorem 3 remain invariant during the procedure of safe guiding. Then we can conclude that the safe guiding will not alter the original optimal policies of (15) applying shaped reward (11) from the work [15].

F. Experimental Details

In each experiment, the LTL tasks are converted into LDGBA that is applied to construct the modular DDPG algorithm. The EP-MDP between E-LDGBA and cl-MDP is synthesized on-fly. As for each actor/critic structure, we used the same feed-forward neural network setting with 3 fully connected layers that has [64, 64, 64] units and ReLu activations. We initiate a Gaussian action distribution for the continuous action space that is parameterized via actors. The parameters of the base reward function, reward shaping, and exploration guiding are set-up as $r_F = 0.9$, $\gamma_F = 0.99$, $\eta_{\Phi} = 1000$, and $r_n = -50$. The training settings and complexity analysis are shown in Table II that provides a comprehensive comparison of time complexity for different tasks using various baselines.

REFERENCES

- [1] R. S. Sutton and A. G. Barto, *Reinforcement learning: An introduction*. MIT press, 2018.
- [2] T. P. Lillicrap, J. J. Hunt, A. Pritzel, N. Heess, T. Erez, Y. Tassa, D. Silver, and D. Wierstra, "Continuous control with deep reinforcement learning," *arXiv preprint arXiv:1509.02971*, 2015.
- [3] J. Schulman, S. Levine, P. Abbeel, M. Jordan, and P. Moritz, "Trust region policy optimization," in *International conference on machine learning*. PMLR, 2015, pp. 1889–1897.
- [4] J. Schulman, F. Wolski, P. Dhariwal, A. Radford, and O. Klimov, "Proximal policy optimization algorithms," *arXiv preprint arXiv:1707.06347*, 2017.
- [5] J. Garcia and F. Fernández, "A comprehensive survey on safe reinforcement learning," *Journal of Machine Learning Research*, vol. 16, no. 1, pp. 1437–1480, 2015.
- [6] M. W. Seeger, S. M. Kakade, and D. P. Foster, "Information consistency of nonparametric gaussian process methods," *IEEE Transactions on Information Theory*, vol. 54, no. 5, pp. 2376–2382, 2008.
- [7] A. K. Akametalu, J. F. Fisac, J. H. Gillula, S. Kaynama, M. N. Zeilinger, and C. J. Tomlin, "Reachability-based safe learning with gaussian processes," in *53rd IEEE Conference on Decision and Control*. IEEE, 2014, pp. 1424–1431.
- [8] J. F. Fisac, A. K. Akametalu, M. N. Zeilinger, S. Kaynama, J. Gillula, and C. J. Tomlin, "A general safety framework for learning-based control in uncertain robotic systems," *IEEE Trans. Autom. Control*, 2018.
- [9] K. Polymenakos, L. Laurenti, A. Patane, J.-P. Calliess, L. Cardelli, M. Kwiatkowska, A. Abate, and S. Roberts, "Safety guarantees for iterative predictions with gaussian processes," in *2020 59th IEEE Conference on Decision and Control (CDC)*. IEEE, 2020, pp. 3187–3193.
- [10] F. Berkenkamp, M. Turchetta, A. P. Schoellig, and A. Krause, "Safe model-based reinforcement learning with stability guarantees," *arXiv preprint arXiv:1705.08551*, 2017.
- [11] T. Koller, F. Berkenkamp, M. Turchetta, and A. Krause, "Learning-based model predictive control for safe exploration," in *2018 IEEE Conference on Decision and Control (CDC)*. IEEE, 2018, pp. 6059–6066.
- [12] A. D. Ames, X. Xu, J. W. Grizzle, and P. Tabuada, "Control barrier function based quadratic programs for safety critical systems," *IEEE Transactions on Automatic Control*, vol. 62, no. 8, pp. 3861–3876, 2016.
- [13] L. Wang, E. A. Theodorou, and M. Egerstedt, "Safe learning of quadrotor dynamics using barrier certificates," in *2018 IEEE International Conference on Robotics and Automation (ICRA)*. IEEE, 2018, pp. 2460–2465.
- [14] R. Cheng, G. Orosz, R. M. Murray, and J. W. Burdick, "End-to-end safe reinforcement learning through barrier functions for safety-critical continuous control tasks," in *Proceedings of the AAAI Conference on Artificial Intelligence*, vol. 33, no. 01, 2019, pp. 3387–3395.
- [15] A. Y. Ng, D. Harada, and S. Russell, "Policy invariance under reward transformations: Theory and application to reward shaping," in *ICML*, vol. 99, 1999, pp. 278–287.
- [16] E. Wiewiora, G. W. Cottrell, and C. Elkan, "Principled methods for advising reinforcement learning agents," in *Proceedings of the 20th International Conference on Machine Learning (ICML-03)*, 2003, pp. 792–799.
- [17] T. Brys, A. Harutyunyan, H. B. Suay, S. Chernova, M. E. Taylor, and A. Nowé, "Reinforcement learning from demonstration through shaping," in *Twenty-fourth international joint conference on artificial intelligence*, 2015.
- [18] F. Memarian, W. Goo, R. Lioutikov, U. Topcu, and S. Niekum, "Self-supervised online reward shaping in sparse-reward environments," *arXiv preprint arXiv:2103.04529*, 2021.
- [19] C. Baier and J.-P. Katoen, *Principles of model checking*. MIT press, 2008.
- [20] D. Aksaray, A. Jones, Z. Kong, M. Schwager, and C. Belta, "Q-learning for robust satisfaction of signal temporal logic specifications," in *Proc. IEEE Conf. Decis. Control*, 2016, pp. 6565–6570.
- [21] H. Venkataraman, D. Aksaray, and P. Seiler, "Tractable reinforcement learning of signal temporal logic objectives," *arXiv preprint arXiv:2001.09467*, 2020.
- [22] N. Piterman, "From nondeterministic buchi and streett automata to deterministic parity automata," in *21st Annual IEEE Symposium on Logic in Computer Science (LICS'06)*. IEEE, 2006, pp. 255–264.
- [23] S. Sickert, J. Esparza, S. Jaax, and J. Křetínský, "Limit-deterministic Büchi automata for linear temporal logic," in *Int. Conf. Comput. Aided Verif.* Springer, 2016, pp. 312–332.
- [24] M. Hasanbeig, N. Yogananda Jeppu, A. Abate, T. Melham, and D. Kroening, "DeepSynth: Program synthesis for automatic task segmentation in deep reinforcement learning," in *AAAI Conference on Artificial Intelligence*. Association for the Advancement of Artificial Intelligence, 2021.
- [25] R. T. Icarte, T. Klassen, R. Valenzano, and S. McIlraith, "Using reward machines for high-level task specification and decomposition in reinforcement learning," in *Int. Conf. Mach. Learn.*, 2018, pp. 2107–2116.
- [26] A. Camacho, R. T. Icarte, T. Q. Klassen, R. A. Valenzano, and S. A. McIlraith, "LTL and beyond: Formal languages for reward function

- specification in reinforcement learning.” in *IJCAI*, vol. 19, 2019, pp. 6065–6073.
- [27] P. Vaezipoor, A. Li, R. T. Icarte, and S. McIlraith, “Ltl2action: Generalizing ltl instructions for multi-task rl,” *arXiv preprint arXiv:2102.06858*, 2021.
- [28] D. Sadigh, E. S. Kim, S. Coogan, S. S. Sastry, and S. A. Seshia, “A learning based approach to control synthesis of Markov decision processes for linear temporal logic specifications,” in *Proc. IEEE Conf. Decis. Control.*, 2014, pp. 1091–1096.
- [29] Q. Gao, D. Hajinezhad, Y. Zhang, Y. Kantaros, and M. M. Zavlanos, “Reduced variance deep reinforcement learning with temporal logic specifications,” in *Proc. ACM/IEEE Int. Conf. Cyber-Physical Syst.*, 2019, pp. 237–248.
- [30] M. Cai, H. Peng, Z. Li, and Z. Kan, “Learning-based probabilistic LTL motion planning with environment and motion uncertainties,” *IEEE Trans. Autom. Control*, 2020, to appear.
- [31] E. M. Hahn, M. Perez, S. Schewe, F. Somenzi, A. Trivedi, and D. Wojtczak, “Omega-regular objectives in model-free reinforcement learning,” in *Int. Conf. Tools Alg. Constr. Anal. Syst.* Springer, 2019, pp. 395–412.
- [32] A. K. Bozkurt, Y. Wang, M. M. Zavlanos, and M. Pajic, “Control synthesis from linear temporal logic specifications using model-free reinforcement learning,” in *Int. Conf. Robot. Autom.* IEEE, 2020, pp. 10 349–10 355.
- [33] M. Cai, S. Xiao, B. Li, Z. Li, and Z. Kan, “Reinforcement learning based temporal logic control with maximum probabilistic satisfaction,” in *Int. Conf. Robot. Autom.* IEEE, 2021, pp. 806–812.
- [34] C. Wang, Y. Li, S. L. Smith, and J. Liu, “Continuous motion planning with temporal logic specifications using deep neural networks,” *arXiv preprint arXiv:2004.02610*, 2020.
- [35] L. Z. Yuan, M. Hasanbeig, A. Abate, and D. Kroening, “Modular deep reinforcement learning with temporal logic specifications,” *arXiv preprint arXiv:1909.11591*, 2019.
- [36] M. Hasanbeig, D. Kroening, and A. Abate, “Deep reinforcement learning with temporal logics,” in *International Conference on Formal Modeling and Analysis of Timed Systems*. Springer, 2020, pp. 1–22.
- [37] M. Cai, M. Hasanbeig, S. Xiao, A. Abate, and Z. Kan, “Modular deep reinforcement learning for continuous motion planning with temporal logic,” *IEEE Robotics and Automation Letters*, vol. 6, no. 4, pp. 7973–7980, 2021.
- [38] M. Alshiekh, R. Bloem, R. Ehlers, B. Könighofer, S. Niekum, and U. Topcu, “Safe reinforcement learning via shielding,” in *Proceedings of the AAAI Conference on Artificial Intelligence*, vol. 32, no. 1, 2018.
- [39] X. Li, Z. Serlin, G. Yang, and C. Belta, “A formal methods approach to interpretable reinforcement learning for robotic planning,” *Sci. Robot.*, vol. 4, no. 37, 2019.
- [40] M. Hasanbeig, A. Abate, and D. Kroening, “Cautious reinforcement learning with logical constraints,” in *Proceedings of the 19th International Conference on Autonomous Agents and MultiAgent Systems*, 2020, pp. 483–491.
- [41] V. I. Paulsen and M. Raghupathi, *An introduction to the theory of reproducing kernel Hilbert spaces*. Cambridge university press, 2016, vol. 152.
- [42] T. Sebastian, B. Wolfram, and D. Fox, “Probabilistic robotics,” *Communications of the ACM*, vol. 45, no. 3, pp. 52–57, 2002.
- [43] F. Bacchus, C. Boutilier, and A. Grove, “Rewarding behaviors,” in *Proceedings of the National Conference on Artificial Intelligence*, 1996, pp. 1160–1167.
- [44] C. J. Watkins and P. Dayan, “Q-learning,” *Mach. Learn.*, vol. 8, no. 3–4, pp. 279–292, 1992.
- [45] J. Kretínský, T. Meggendorfer, and S. Sickert, “Owl: A library for ω -words, automata, and LTL,” in *Autom. Tech. Verif. Anal.* Springer, 2018, pp. 543–550. [Online]. Available: https://doi.org/10.1007/978-3-030-01090-4_34
- [46] R. Durrett and R. Durrett, *Essentials of stochastic processes*. Springer, 1999, vol. 1.
- [47] V. Mnih, K. Kavukcuoglu, D. Silver, A. A. Rusu, J. Veness, M. G. Bellemare, A. Graves, M. Riedmiller, A. K. Fidjeland, G. Ostrovski *et al.*, “Human-level control through deep reinforcement learning,” *Nature*, vol. 518, no. 7540, pp. 529–533, 2015.
- [48] T. Haarnoja, A. Zhou, P. Abbeel, and S. Levine, “Soft actor-critic: Off-policy maximum entropy deep reinforcement learning with a stochastic actor,” in *International Conference on Machine Learning*. PMLR, 2018, pp. 1861–1870.
- [49] C. Rasmussen and C. Williams, *Gaussian Processes for Machine Learning*, ser. Adaptive Computation and Machine Learning. Cambridge, MA, USA: MIT Press, Jan. 2006.
- [50] Q. Nguyen and K. Sreenath, “Exponential control barrier functions for enforcing high relative-degree safety-critical constraints,” in *2016 American Control Conference (ACC)*. IEEE, 2016, pp. 322–328.
- [51] W. Xiao and C. Belta, “High order control barrier functions,” *IEEE Transactions on Automatic Control*, 2021.
- [52] A. Agrawal and K. Sreenath, “Discrete control barrier functions for safety-critical control of discrete systems with application to bipedal robot navigation,” in *Robotics: Science and Systems*, 2017.
- [53] M. Srinivasan, A. Dabholkar, S. Coogan, and P. Vela, “Synthesis of control barrier functions using a supervised machine learning approach,” *arXiv preprint arXiv:2003.04950*, 2020.
- [54] A. Robey, H. Hu, L. Lindemann, H. Zhang, D. V. Dimarogonas, S. Tu, and N. Matni, “Learning control barrier functions from expert demonstrations,” in *2020 59th IEEE Conference on Decision and Control (CDC)*. IEEE, 2020, pp. 3717–3724.
- [55] S. W. Squyres, A. H. Knoll, R. E. Arvidson, J. W. Ashley, J. Bell, W. M. Calvin, P. R. Christensen, B. C. Clark, B. A. Cohen, P. De Souza *et al.*, “Exploration of victoria crater by the mars rover opportunity,” *Science*, vol. 324, no. 5930, pp. 1058–1061, 2009.